1   **FOXO1 represses *Sprouty2* and *Sprouty4* expression**

2   **in endothelial cells to promote arterial specification and vascular remodeling**

3   **in the mouse yolk sac**

4

5   Nanbing Li-Villarreal*, Rebecca Lee Yean Wong*, Monica D. Garcia*, Ryan S. Udan, Ross A.

6   Poché, Tara L. Rasmussen, Alexander M. Rhyner, Joshua D. Wythe, and Mary E. Dickinson**

7

8   Department of Molecular Physiology & Biophysics, Baylor College of Medicine. One Baylor

9   Plaza, Houston, Texas 77030.

10
11   *   Authors who contributed equally to the work

12   **   Correspondence: mdickins@bcm.edu

13

14 **ABSTRACT**

15 The establishment of a functional circulatory system is required for post-implantation

16 development during murine embryogenesis. Previous studies in loss of function mouse models

17 have shown that FOXO1, a Forkhead family transcription factor, is required for yolk sac vascular

18 remodeling and survival beyond embryonic day (E) 11. Here, we demonstrate that loss of

19 *FoxO1* in E8.25 endothelial cells results in increased *Sprouty2* and *Sprouty4* transcripts,

20 reduced expression of arterial genes, and decreased *Flk1/Vegfr2* mRNA levels without affecting

21 overall endothelial cell identity, survival, or proliferation. Using a *Dll4-BAC-nlacZ* reporter line,

22 we found that one of the earliest expressed arterial genes, *Delta like 4* (*Dll4*), is significantly

23 reduced in the yolk sac of *FoxO1* mutants without being substantially affected in the embryo

24 proper. We show that in the yolk sac, FOXO1 not only binds directly to a subset of previously

25 identified *Sprouty2* gene regulatory elements (GREs), as well as newly identified, evolutionarily

26 conserved *Sprouty4* GREs, but can also repress their expression. Additionally, over expression

27 of *Sprouty4* in transient transgenic embryos largely recapitulates reduced expression of arterial

28 genes seen in endothelial *FoxO1* mutant mouse embryos. Together, these data reveal a novel

29 role for FOXO1 as a key early transcriptional repressor controlling both pre-flow arterial

30 specification and subsequent vessel remodeling within the murine yolk sac.

31

32

33 **INTRODUCTION**

34   During early development the mammalian embryo requires a functional circulatory

35 system to distribute oxygen, nutrients, and hormones. The mammalian heart is the first organ to

36 form and function within this early embryo, along with the first arteries and veins that arise de

37 novo via vasculogenesis (Fish and Wythe, 2015, Risau, 1994, Risau and Flamme, 1995, Chong

38 et al., 2011). Primitive erythrocytes form in the blood islands of the extra-embryonic yolk sac

39 (YS), and are drawn into circulation as the heart begins to beat around embryonic day (E) 8 in

40 the mouse embryo (Lucitti et al., 2007, Palis, 2014, Ji et al., 2003). A complete circulatory loop

41 between the embryo and the extra-embryonic YS is evident shortly after the onset of cardiac

42 contractions, with blood flowing through the dorsal aorta to the vitelline (omphalomesenteric)

43 artery (VA), through the YS capillary plexus, and back through the vitelline (omphalomesenteric)

44 vein (VV) to the sinus venosus of the heart. Circulation through the YS is the main circulatory

45 loop until the chorion-allantoic placenta connections develop later around E9.

46   A key finding several years ago showed that arterial-venous (AV) identity is established

47 prior to the onset of blood flow in the early mouse embryo (Herzog et al., 2005, Chong et al.,

48 2011, Aitsebaomo et al., 2008, Wang et al., 1998, Adams et al., 1999). Others have since

49 shown that some aspects of AV identity are plastic, as they can be influenced by changes in

50 blood flow and hemodynamics (le Noble et al., 2004, le Noble et al., 2005, Wragg et al., 2014).

51 Extensive work in zebrafish has shown that AV specification depends on differential responses

52 to VEGF signaling through the tyrosine kinase receptor VEGFR2/Flk1, high levels of which

53 activate the MEK/ERK kinase cascade in arterial cells and PI3K/AKT signaling in venous cells

54 (Fish and Wythe, 2015, Covassin et al., 2006, Weinstein and Lawson, 2002). In the arterial

55 endothelium, VEGFR2 signaling stimulates the Notch pathway, which in turn promotes an

56 arterial identity while simultaneously repressing a venous fate (Weinstein and Lawson, 2002,

57 Krebs et al., 2010, Lawson et al., 2001, Lawson et al., 2002, Liu et al., 2003, Shutter et al.,

58 2000, Swift and Weinstein, 2009, Siekmann and Lawson, 2007, Krebs et al., 2000, Duarte et al.,

59   2004, Lobov et al., 2007). VEGF upregulates expression of *Delta-like 4 (Dll4),* which encodes a

60   ligand for the Notch family of transmembrane receptors. *Dll4* is the earliest Notch ligand

61   expressed in arterial cells in the early mouse embryo (Shutter et al., 2000, Mailhos et al., 2001,

62   Wythe et al., 2013, Cleaver and Krieg, 1998, Chong et al., 2011), and is essential for AV

63   patterning (Krebs et al., 2000, Gale et al., 2004, Duarte et al., 2004). Expression of *Dll4*

64   depends on the activation of ETS transcription factors, downstream of VEGF signaling (Wythe

65   et al., 2013, Fish et al., 2017) and *Dll4* mRNA expression can be increased by shear stress

66   (Masumura et al., 2009, Obi et al., 2009). However, the expression of *Dll4* and a few other

67   select arterial markers prior to, and independent of, the onset of blood flow (Chong et al., 2011,

68   Wang et al., 1998) suggests flow-independent mechanisms regulate arterial specification.

69   Vegfr2 also upregulates expression of the main endothelial cell surface receptor for Dll4, Notch1

70   (Lawson et al., 2002). Notch itself is activated by blood flow and the strength of this signal

71   depends on the magnitude of shear stress (Masumura et al., 2009, Mack et al., 2017). Notch

72   regulates cell junctions, cell cycle arrest, and induces an arterial gene expression program via a

73   connexin37 (*Gja4*)/p27^{Kip1} (*Cdkn1B*) pathway (Mack et al., 2017, Su et al., 2018, Fang et al.,

74   2017). Critically, both Vegfr2 and Notch1 are thought to act as mechanosensors, likely linking

75   arterial specification of ECs and hemodynamic feedback via blood flow to re-enforce and solidify

76   their arterial identity (Mack et al., 2017, Tzima et al., 2005, Mack and Iruela-Arispe, 2018, Shay-

77   Salit et al., 2002).

78   Forces exerted by blood flow play a clear role in AV specification, and also influence

79   vessel morphogenesis and remodeling in the early embryo (Fang et al., 2017, Masumura et al.,

80   2009, le Noble et al., 2004, Chong et al., 2011, Hwa et al., 2017). Hemodynamic force is both

81   necessary and sufficient to remodel the high-resistance mouse YS capillary plexus into a more

82   complex hierarchical network with a large caliber VA and VV progressively leading to smaller

83   diameter vessels (Lucitti et al., 2007). Our lab has shown that murine yolk sac vessel

84   remodeling depends on both vessel fusion and EC migration (Udan et al., 2013). Interestingly,

85   live imaging studies showed distinct differences in how arterial and venous cells respond to

86   changes in hemodynamic force (Udan et al., 2013, Kondrychyn et al., 2020, Goetz et al., 2014).

87   These data suggest that pathways that control AV identity, which can be regulated by blood

88   flow, may also influence physical responses of ECs to blood flow such as migration and motility

89   that facilitate vessel remodeling.

90   Despite the knowledge that has been gained regarding the mechanisms regulating

91   arterial-venous identity and the discovery of mechanosensors that are required for ECs to sense

92   blood flow, a full understanding of these mechanistic pathways is yet to be realized. A recent

93   analysis estimates that approximately 6% of genes in the genome (~1200) may be required

94   during early cardiovascular development (E9.5-E12.5) (Dickinson et al., 2016). One such gene,

95   and the focus of this study, is *FoxO1 (Forkhead box protein O1)*. *Forkhead domain class O*

96   *transcription factors (FOXOs)* integrate different cellular signaling pathways to regulate cellular

97   homeostasis (Paik et al., 2007, Huang and Tindall, 2007, Jiramongkol and Lam, 2020). *Daf-*

98   *16/FoxO* was originally identified as a regulator of dauer formation in *C. elegans* (Albert et al.,

99   1981) and was later shown to control longevity by sensing environmental cues such as

100   hormones, nutrient availability, oxidative stress, and energy metabolism via signaling through

101   the insulin, AKT/mTor, JNK and AMPK pathways (Sun et al., 2017). Several studies have since

102   established that *FoxO1* is also required for normal embryonic development in mice.

103   Homozygous null *FoxO1* embryos display a primitive yolk sac vasculature, pericardial edema,

104   and disorganized embryonic vessels by E9.5, resulting in lethality by E11.5 (Furuyama et al.,

105   2004, Dharaneeswaran et al., 2014, Hosaka et al., 2004, Sengupta et al., 2012, Wilhelm et al.,

106   2016, Ferdous et al., 2011). Further analysis showed that loss of *FoxO1* in the endothelium, but

107   not the myocardium, phenocopied germline loss of *FoxO1* (Sengupta et al., 2012),

108   demonstrating the cell autonomous requirement for FOXO1 in the embryonic vasculature.

109   Follow-up studies have since found that FOXO1 controls a variety of different processes in

110   endothelial cells (ECs), including, but not limited to EC proliferation and metabolism (Wilhelm et

111   al., 2016), endothelial barrier function (Beard et al., 2020), sprouting angiogenesis (Kim et al.,

112   2019, Fukumoto et al., 2018, Dang et al., 2017), autophagy (Zhang et al., 2019), EC growth

113   (Riddell et al., 2018, Rudnicki et al., 2018) and migration (Niimi et al., 2017). Despite these

114   studies, the exact function that FOXO1 plays in the early vasculature remains elusive. Given

115   that FOXO1 activity can be modulated in response to fluid shear stress (Chlench et al., 2007,

116   Dixit et al., 2008), combined with our studies showing that hemodynamic force is necessary and

117   sufficient for early vascular remodeling (Lucitti et al., 2007, Udan et al., 2013), and the growing

118   evidence for FOXO1 in cell migration and sprouting angiogenesis (Fosbrink et al., 2006, Niimi et

119   al., 2017, Kim et al., 2019), we define the requirement for FOXO1 in the remodeling vasculature

120   of the early embryonic yolk sac.

121   Herein, we demonstrate a novel role for FOXO1 in regulating AV identity in the murine

122   YS vasculature. Using conditional, endothelial-specific *FoxO1* loss-of-function mutants, we

123   identified a significant down regulation of arterial gene expression in the mouse yolk sac prior to

124   the onset of blood flow. We also detected a significant reduction in *Vegfr2/Flk1* transcripts, but

125   normal expression levels for other pan-endothelial genes such as *Pecam1*, indicating that the

126   formation of ECs is not disrupted but rather VEGF signaling is affected. Using a novel *Dll4*

127   arterial reporter line, we showed that *FoxO1* is required for *Dll4* expression in the murine yolk

128   sac, but not in the embryo proper. Further analysis showed that FOXO1 represses expression

129   of *Sprouty* genes, which encode inhibitors of Raf/MEK/ERK signaling downstream of FGF and

130   VEGF receptor activation. Sprouty factors also modulate angiogenesis by negatively regulating

131   small vessel branching, as well as repressing endothelial cell migration (Gong et al., 2013,

132   Wietecha et al., 2011, Lee et al., 2001). While some have shown that FOXO1 positively

133   regulates *Sprouty* gene expression (Paik et al., 2007), our studies demonstrate that *FoxO1* loss

134   increased *Sprouty2* and *4* mRNA levels, suggesting that FOXO1 represses *Sprouty2/4* in the

135   murine yolk sac. We went on to find that *Sprouty4* overexpression throughout the yolk sac and

136   embryo profoundly altered arterial gene expression in the yolk sac but, similar to early FoxO1

137   loss, had an insignificant effect on these transcripts in the embryo proper. Taken together, these

138   data highlight a novel role for FOXO1 in regulating arteriovenous specification in the early yolk

139   sac and reveal a new mechanism wherein FOXO1 represses *Sprouty* gene expression and

140   downstream signaling in the endothelium.

141

142   **Results:**

143   **Defective yolk sac vascular remodeling in *FoxO1*ECKO embryos is not due to abnormalities**

144   **in hemodynamic force or allantois defects**

145   To define the role of FOXO1 in ECs within the early embryo, we conditionally ablated

146   *FoxO1* in the endothelium by crossing *FoxO1*^{flox} mice (Paik et al., 2007) with *Tie2-Cre*

147   transgenic mice, in which Cre recombinase is expressed in endothelial and hematopoietic cells

148   and progenitors starting at E7.5 (Kisanuki et al., 2001). The efficiency of the *Tie2-Cre* mediated

149   recombination of the *FoxO1*^{flox} allele was confirmed by qRT-PCR, which showed over 60%

150   reduction in *FoxO1* mRNA in CKO yolk sacs compared to control littermates at E8.5 (Figure

151   1A). We observed gross phenotypes similar to previous reports (Figure 1B and C and S1A and

152   B) (Sengupta et al., 2012, Furuyama et al., 2004, Hosaka et al., 2004). There were no visible

153   differences in vascular morphology or embryo size between control (*Tie2-Cre*$^{+/+}$*;FoxO*$^{+/flox}$) and

154   endothelial conditional knockout embryos (*Tie2-Cre*$^{+/tg}$*;FoxO1*$^{flox/flox}$*,* hereafter referred to as

155   *FoxO1*^{ECKO}) at E8.5 (Figures 1D and E). However, at E9.5 and E10.5, while the primitive

156   vascular plexus of the control yolk sac had remodeled into a hierarchy of large caliber vessels

157   iteratively branching into smaller diameter capillaries, *FoxO1*^{ECKO} yolk sacs retained a primitive

158   vascular plexus (Figures 1F-I). *FoxO1*^{ECKO} embryos stained with anti-CD31 antibodies showed a

159   thinner and less branched vitelline vein and artery compared to controls (Figure 1J). At E9.5,

160   mutant embryos were reduced in overall size compared to control littermates (Figures 1F and

161   G), and this became more evident at E10.5 (Figures 1B-C, H-I). Additionally, in both E9.5 (not

162   shown) and E10.5 *FoxO1*^{ECKO} embryos (Figure 1I), the pericardial sac was enlarged, and blood

163   was abnormally pooled in the heart. Overall, phenotypes in *FoxO1* mutant embryos are highly

164   reproducible and our observations align well with previously published studies (Sengupta et al.,

165   2012, Furuyama et al., 2004, Hosaka et al., 2004).

166   The appearance of pericardial edema in *FoxO1^{ECKO}* embryos is suggestive of heart

167   failure and compromised circulation. To determine if and when blood flow was impaired, we

168   crossed a primitive erythrocyte transgenic fluorescent reporter line, *ε-globin-KGFP* (Dyer et al.,

169   2001) into the *FoxO1^{ECKO}* background. Live imaging of cultured embryos and high-speed

170   confocal microscopy was used to track individual KGFP labeled erythroblasts to determine

171   blood velocity (Figure 2) (Jones et al., 2004). At E8.5, both control and *FoxO1^{ECKO}* embryonic

172   vessels were filled with blood and erythrocytes moved with a steady directional flow with similar

173   periodicity and velocity (Figures 2A, B, E, and G). By E9.5, control embryos had clearly

174   remodeled vessels, blood flow velocity greater than 700 μm/s, and a defined wave pattern with

175   periodicity of 400 ms (Figures 2C and F).   However, *FoxO1^{ECKO}* embryos vessels were not

176   remodeled, and blood flow had a significantly lower velocity, with a poorly defined wave pattern

177   (Figures 2D and H). Quantification of blood velocity (Figures 2I-J) and heart rate (Figures 2K-L)

178   revealed no statistical difference in E8.5 control and *FoxO1^{ECKO}* embryos (Figures 2I and K).

179   However, by E9.5, blood velocity and heart rate were significantly decreased in *FoxO1^{ECKO}*

180   embryos (Figures 2J and L), indicating heart failure was occurring in embryos with un-

181   remodeled vessels. Thus, flow initiates normally in *FoxO1^{ECKO}* embryos and flow abnormalities

182   are not detected until after defects in vessel remodeling are evident. Given these results, we

183   restricted our analysis, whenever possible, to E8.25-E8.5 embryos so that poor blood flow did

184   not influence our observations.

185   A previous report on the role of *FoxO1* in placental development described phenotypes

186   including swollen or hydropic allantois, failed chorion-allantoic fusion, and increased cell death

187   in the allantois (Ferdous et al., 2011). Since the previous study was conducted in germline

188   *FoxO1* null embryos, we examined the allantois in global null and *FoxO1^{ECKO}* mutants. While

8

189   germline *FoxO1* mutants exhibited partially penetrant defects in allantois formation and fusion,

190   these phenotypes were not evident in *FoxO1*[ECKO] embryos at E9.5 (Table 1). However, both

191   germline and *FoxO1*[ECKO] embryos show defects in yolk sac vascular remodeling, heart failure

192   phenotypes, and lethality by E11.5. Taken together, these results support a cell autonomous

193   requirement for FOXO1 in yolk sac vessel remodeling and suggest that published cardiac and

194   blood flow defects are secondary to the impaired remodeling of yolk sac vasculature.

195

196   **FOXO1 is necessary to maintain *Flk1/Vegfr2* expression in E8.25 embryos**

197   To further assess the effect of endothelial-specific *FoxO1* deletion in the developing embryo, we

198   examined transcript levels of genes normally expressed in blood vessels by qRT-PCR within

199   *FoxO1*[ECKO] E8.25 yolk sacs. We focused these experiments at E8.25 to avoid potential

200   complications of later stage heart failure. We observed a significant decrease in *Flk1/Vegfr2*

201   expression in *FoxO1*[ECKO] yolk sacs, while other pan-endothelial markers such as *Pecam1*, *Tie2*,

202   *VE-Cadherin*, *Flt1/Vegfr1,* and *Cx43* were not significantly affected (Figure 3A). Immuno-

203   labeling of endogenous *Flk1* showed a similar reduction in expression in *FoxO1*[ECKO] yolk sac

204   endothelial cells at E8.25, while Pecam1 (CD31) expression – a pan endothelial cell marker –

205   appeared unaffected (Figure 3B). We further confirmed the reduction in *Flk1* expression using

206   magnetic-activated cell sorting (MACS) to isolate CD31$^+$ ECs from E8.25 WT and *FoxO1*

207   germline deletion mutant yolk sacs. CD31$^+$ yolk sac ECs showed seven-fold higher expression

208   of *Pecam1* mRNA (which encodes CD31) than whole yolk sacs (isolated separately then

209   combined) and approximately thirty-fold higher than the non-endothelial population (CD31$^-$),

210   demonstrating the enrichment of endothelial cells via MACS (Figure 3C). To compare WT and

211   mutant endothelial cells, we assayed transcript levels of both *Pecam1* (CD31) and *Flk1* (Vegfr2)

212   in the CD31$^+$ populations. *Pecam1* levels were comparable between WT and mutant endothelial

213   cells, whereas *Flk1* was significantly reduced in the germline mutant endothelial cells (Figure 3D

214   and E). Finally, we examined *Flk1* expression using a transgenic reporter, *Flk1-H2B::YFP*

215   (Fraser et al., 2005), which labels endothelial cell nuclei. At E8.25, YFP$^+$ endothelial nuclei were

216   evenly dispersed throughout the vascular plexus of control yolk sacs, however, the number of

217   YFP$^+$ nuclei within the *FoxO1^{ECKO}* yolk sacs were significantly reduced (Figure 3F). The total

218   number of DAPI$^+$ nuclei was unchanged. Nuclear segmentation and quantification of the

219   average YFP$^+$ cell density revealed a significant reduction in the number of YFP$^+$ cells in

220   *FoxO1^{ECKO}* yolk sacs compared to controls (Figure 3G). To determine if the reduction in YFP$^+$

221   cells was due to a difference in apoptosis or proliferation, *FoxO1^{ECKO}* litters positive for the *Flk1-*

222   *H2B-YFP* reporter were immunostained for phospho-histone 3 (PH3) or Caspase 3 (Figure 3H

223   and I). We found that neither cell proliferation nor apoptosis within the yolk sac differed

224   significantly between control and *FoxO1^{ECKO}* embryos (Figures 3 H, I, S2A-D). Since the mRNA

225   expression of pan-endothelial markers was not decreased, but Flk1 transcripts and protein were

226   reduced, we concluded that the low density in YFP$^+$ cells is not due to reduced EC numbers, but

227   rather reduced expression of the *Flk1* reporter. Collectively, these data indicate that FOXO1 is

228   required to maintain cell autonomous *Flk1/Vegfr2* expression in ECs, but not required for the

229   formation, proliferation or survival of ECs or the expression of other pan-endothelial markers.

230

231   **FOXO1 is required to regulate arterial gene expression in the yolk sac vasculature**

232   Given the reduction in *Flk1/Vegfr2* expression in E8.25 embryos, and the critical role of VEGF-

233   VEGFR2 signaling in establishing arteriovenous identity in the early embryonic endothelium, we

234   next examined other markers of AV specification (Figure 4A). Previously, Furuyama *et al.*

235   showed reduced expression of the arterial-enriched transcripts *Cx40, Cx37, eNOS, and*

236   *EphrinB2* in the yolk sacs of E9.5 *FoxO1^{ECKO}* mutants compared to control littermates

237   (Furuyama et al., 2004), but given the changes in blood flow that we observed in E9.5

238   *FoxO1^{ECKO}* embryos, we were interested to determine if expression of these markers was

239   affected earlier. Indeed, these genes were significantly reduced in *FoxO1^{ECKO}* yolk sacs at

240   E8.25 compared to controls (Figure 4A). In addition, we found a significant reduction in

10

241 transcript levels of Notch family members, including *Notch1*, *Hey1*, *Hey2*, *Jagged1* and *Dll4*,

242 which are required for arterial specification (Gridley, 2010, Duarte et al., 2004, Xue et al., 1999,

243 Fischer et al., 2004). Furthermore, *Neuropilin1*, which encodes a co-receptor for VEGFR2 and is

244 required for arterial specification, was also downregulated, whereas its venous counterpart,

245 *Neuropilin2*, remained unchanged (Herzog et al., 2001). Additional venous markers, *Coup-TFII*

246 *(NR2F2)* and *EphB4*, showed a modest decrease, or no significant change, respectively (Wang

247 et al., 1998, You et al., 2005). The endodermal marker *Afp* was also unchanged (Figure 4A)

248 (Dziadek and Adamson, 1978), showing further that gene transcription changes were confined

249 to markers in the arterial endothelium. These results demonstrate that FOXO1 is required for

250 normal expression of early arterial genes, but is dispensable for venous identity, in the murine

251 yolk sac.

252   To determine if reduced transcript levels of arterial-specific genes correlated with

253 decreased expression of their respective proteins in $FoxO1^{ECKO}$ yolk sacs, immunofluorescence

254 was performed on sectioned yolk sacs at E8.25. Confocal imaging of Cx37 and Cx40 revealed

255 an overall reduction in the number of connexin-positive puncta in $FoxO1^{ECKO}$ yolk sacs when

256 compared to controls (Figure S3A and B). Similarly, we observed decreased eNOS expression

257 within the vascular plexus in $FoxO1^{ECKO}$ yolks sacs compared to controls (Figure 4B). These

258 data, in addition to previous gene expression analysis, indicate that FOXO1 within the

259 developing endothelium is necessary for the regulation of arterial endothelial cell identity.

260

261 **Characterization of arterial defects in $FoxO1^{ECKO}$ and germline mutants using the *Dll4-***

262 ***BAC-nlacZ* reporter**

263 Thus far, our phenotypic, transcriptional, and immunolabeling studies support a role for FOXO1

264 as a regulator of vascular remodeling, *Flk1* expression and arterial specification of endothelial

265 cells within the yolk sac. To further analyze the arterial specification defects in $FoxO1^{ECKO}$

266 mutants, we examined the spatial expression of one of the earliest markers of arterial identity

267   (Chong et al., 2011, Wythe et al., 2013), *Dll4*, using a transgenic reporter line, *Dll4-BAC-nlacZ*,

268   that faithfully recapitulates endogenous *Dll4* expression (Herman et al., 2018). E8.25 *FoxO1^ECKO*

269   embryos carrying the nuclear-localized β-galactosidase reporter were compared with control

270   littermates (Figure 5). In E8.25 control embryos, *Dll4-BAC-nlacZ* reporter activity was observed

271   in the dorsal aorta (DA), endocardium (EC), and nascent umbilical artery (UA) within the

272   allantois (Figure 5A and S4A). LacZ positive nuclei were also detected within the YS in and

273   around the vitelline artery and arterioles (Figure 5A, red arrows). *FoxO1^ECKO* yolk sacs exhibited

274   a similar LacZ expression pattern spatially, albeit with reduced intensity (Figure 5B), consistent

275   with our transcript analysis showing reduced *Dll4* mRNA expression in the *FoxO1^ECKO* yolk sacs

276   (Figure 4A and 5C). However, unlike in the yolk sac, nLacZ expression was only slightly

277   reduced in the embryo proper of *FoxO1^ECKO* mutants (Figure S4B compared to S4A, Figure 5C).

278   To determine if the differences in nLacZ reporter expression between the yolk sac and embryo

279   was influenced by Cre-mediated recombination in our conditional knockout studies, we

280   examined the activity of the *Dll4* LacZ reporter in germline *FoxO1* mutants. Figures 4SE and F

281   show representative images of anterior views of the embryos, while Figure 5D and E show

282   posterior views. Results similar to the findings in the *FoxO1^ECKO* embryos were observed, but

283   with even greater decreases in reporter expression between control (5D red arrows) and null

284   (5E red arrows) yolk sacs and embryos. Endogenous *Dll4* expression in the embryo proper and

285   the yolk sac showed a small, but significant decrease in endogenous *Dll4* expression between

286   control and *FoxO1* null embryos. Comparatively, a dramatic reduction in *Dll4* expression was

287   observed in the *FoxO1* null yolk sacs compared to wildtype controls (Figure 5F).

288   By E9.5, nLacZ reporter expression was detected in the arterial tree in the yolk sac,

289   particularly in the VA and within the arterioles (Figure 5G and 5G inset). Consistent with the

290   E8.25 results, we found Dll4 expression reduced in E9.5 *FoxO1^ECKO* yolk sacs (Figure 5H and

291   5H inset) but strong expression in vessels within control and *FoxO1^ECKO* embryos (Figures 5I

292   and J). Germline null embryos showed similar nLacZ activity compared to controls (Figure 5K),

12

293   but reporter expression was not detectable in null yolk sacs, despite the strong expression seen

294   in the embryo (5L). Isolated embryos confirmed LacZ expression in both control (5M) and null

295   embryos (5N). Additional analysis of *Dll4* reporter expression confirmed previous reports of

296   vascular defects in *FoxO1* mutants, including within the intersomitic vessels, cranial vessels and

297   dorsal aorta (5I, J,M, and N, red arrows) (Hosaka et al., 2004, Ferdous et al., 2011,

298   Dharaneeswaran et al., 2014). Collectively, our results indicate that FOXO1 plays a critical and

299   early role in the regulation of *Dll4* expression, a key factor in determining arterial identity, within

300   the extra-embryonic arteries of the yolk sac, but does not appear to be required for *Dll4*

301   expression within the embryo proper.

302

303   ***FoxO1* deletion in endothelial cells upregulates *Sprouty2/4* expression**

304   We uncovered a novel role for FOXO1 in the establishment of arterial identity, but neither *Flk1*

305   nor *Dll4* contain known binding sites for FOXO1, so we examined expression levels of

306   previously validated FOXO1 direct transcriptional targets in the endothelium: adrenomedullin

307   (*Adm)*, BMP binding endothelial regulator (*Bmper*), *eNOS*, *Sprouty2*, and *Vcam1* (Potente et al.,

308   2005, Ferdous et al., 2011). qRT-PCR analysis in *FoxO1^{ECKO}* yolk sacs at E8.25 (Figure 6A)

309   revealed no significant reduction in *Adm* or *Bmper,* but a significant downregulation in *eNOS*

310   and *Vcam1*, as previously described in other tissues (Potente et al., 2005, Ferdous et al., 2011).

311   Interestingly, *FoxO1^{ECKO}* yolk sacs showed significantly increased *Sprouty2* expression (Figure

312   6A). Subsequent analysis showed that in addition to *Sprouty2*, *Sprouty4* was also upregulated

313   in mutant yolk sacs compared to controls, while *Sprouty1* and *3* levels were unchanged (Figure

314   6B). We focused our subsequent analysis on the Sprouty factors because Sprouty4 over-

315   expression had been shown to inhibit angiogenesis in the yolk sac (Lee et al., 2001) and the

316   upregulation of *Sprouty* transcripts led us to hypothesize that FOXO1 may act as a direct

317   repressor of *Sprouty* gene expression.

318   In keeping with the idea that FOXO1 may normally repress *Sprouty 2/4* transcription, we

319   examined endogenous mRNA levels of *FoxO1* and *Sprouty1-4* in wildtype E8.25-8.5 yolk sacs.

320   This analysis revealed that *Sprouty2/4* expression is much lower than *FoxO1*, *Sprouty1* or

321   *Sprouty3* (Figure 6C). To expand and confirm our previous analysis of *Sprouty 2/4* expression,

322   we examined *Sprouty 2/4* transcripts in CD31$^+$ and CD31$^-$ MACS-sorted ECs from germline

323   *FoxO1* mutants and controls (Figure 3D). For *Sprouty2*, we observed increased expression in

324   CD31$^+$ cells, but there was no change in non-endothelial cells from null mutant yolk sacs (Figure

325   6D). Surprisingly, while *Sprouty4* transcripts increased in ECs of null yolk sacs, transcripts were

326   decreased in non-endothelial cells. These data suggest that FOXO1 may act as both a

327   transcriptional repressor or activator in adjacent tissues in the yolk sac, depending on the cell

328   identity or transcriptional target.

329

330   **FOXO1 directly binds to endogenous *Sprouty2/4* promoters and represses *Sprouty2/4***

331   **transcription**

332   FOXO1 is known to regulate *Sprouty2* mRNA expression in liver endothelial cells, and *in vivo*

333   chromatin immunoprecipitation (ChIP) experiments confirmed that FOXO1 occupies four

334   conserved FOXO binding elements within the murine *Sprouty2* locus (Paik et al., 2007). The

335   first FOXO1 binding site (Figure S5A) is located ~4kb upstream of the transcriptional start site

336   (TSS) of murine *Sprouty2,* and the second DNA-binding site is within exon 2 (Figure 7A). The

337   third and fourth FOXO1 binding sites are located ~5kb and 7kb downstream of the TSS,

338   respectively (Figure 7A). Paik, et al. showed that FOXO1 interacts with these loci to activate

339   *Sprouty2* in the liver, but it was unknown whether FOXO1 utilizes the same binding sites to

340   repress *Sprouty2* in the yolk sac. To determine if FOXO1 occupies any of these four identified

341   binding sites in the murine yolk sac, we performed ChIP-PCR using pooled E8.25 yolk sacs. As

342   shown in Figure 7B, FOXO1 occupancy was significantly enriched at the -4051, +5060, and

343   +6972 regions compared to IgG control. FOXO1 enrichment was not observed at the +4479

14

344   region. This demonstrates that during early yolk sac blood vessel development, FOXO1 binds

345   *Sprouty2* at regulatory regions -4051, +5060, and +6972 and supports the context-dependent

346   function of FOXO1.

347   Next, we generated luciferase reporter constructs containing ~2kb of the murine

348   *Sprouty2* promoter, or specific regulatory regions harboring FOXO1 binding sites, and

349   measured transcriptional activity in cultured mammalian cells (Figure S5B). To avoid potential

350   confounds in our analysis from endogenous FOXO1, the human lung cancer cell line H1299

351   was chosen since FOXO1 protein expression is undetectable in this line (Zhao et al., 2010).

352   Overexpression of *FoxO1* (*FLAG::FoxO1*) significantly repressed luciferase activity of the

353   promoter construct containing the -4051 FOXO1 binding site in a dose dependent manner.

354   Furthermore, co-transfecting the same reporter construct along with a FOXO1 cDNA without

355   a DNA binding domain abolished this transcriptional repression (Figure 7C). In contrast,

356   FOXO1 did not significantly repress luciferase activity in the constructs containing either the

357   +4479/5060 or +6972 *Sprouty2* regulatory regions. These results suggest that FOXO1 directly

358   downregulates *Sprouty2* expression via the -4051 site in its promoter.

359   To determine if this role for FOXO1 is evolutionarily conserved, we examined the

360   *Sprouty4* locus for conserved FOXO1 DNA-binding motifs. Two putative binding sites, which

361   were conserved in at least three vertebrate genomes (mammalian and non-mammalian),

362   were identified +8755 bp and +14942 bp downstream of the *Sprouty4* TSS (Figure 7D).

363   FOXO1 ChIP-PCR using E8.25 yolk sac chromatin showed a significant enrichment of

364   FOXO1 occupancy in both regulatory regions (Figure 7E). Luciferase assays in H1299 cells

365   also showed that these same sites were required for wildtype FOXO1 dose-dependent

366   repression of reporter activity (Figure 5F; S5E). Taken together, data from the *Sprouty* mRNA

367   expression analysis, as well as ChIP and luciferase assays, demonstrated that FOXO1

368   directly repressed *Sprouty2* and *Sprouty4* transcription in the E8.25 murine yolk sac via

369   known and newly identified conserved DNA-binding sites.

370

Transient overexpression of *Sprouty4* in endothelial cells phenocopies conditional loss-of-function *FoxO1* mutants

Given the fact that *Sprouty2* and *Sprouty4* are known to have anti-angiogenic functions (Taniguchi et al., 2009, Wietecha et al., 2011, Lee et al., 2001), and our data herein show that FOXO1 directly represses *Sprouty2/4* expression in the yolk sac, we hypothesized that FOXO1 promotes arterial gene expression by repressing *Sprouty2/4.* It had previously been shown that adenovirus-mediated overexpression of *Sprouty4* in developing embryos inhibited sprouting and branching of small vessels in the embryo proper and vessel remodeling in the yolk sac (Lee et al., 2001). To test whether *Sprouty4* overexpression could recapitulate the *FoxO1* loss-of-function phenotype, we utilized a well-characterized *Flk1* promoter-enhancer construct (Kappel et al., 1999, Ronicke et al., 1996, Fraser et al., 2005) to transiently overexpress *Sprouty4* in the endothelial cells of the mouse embryo and YS beginning at E7.5. To track transgene expression, a H2B::YFP reporter was inserted downstream to enable identification of YFP⁺ transgenic embryos (schematized in Figure 8A). E8.25 or E9.5 yolk sacs of YFP⁺ transgenic embryos (n=3) showed poorly remodeled vasculature, as their vessels remained as a primitive vascular plexus, while at E9.5 non-transgenic embryos had a normally developed vitelline artery with large caliber vessels branching into smaller diameter capillaries (Figure 8B). The lack of yolk sac vascular remodeling in the transient transgenic *Flk1-Sprouty4* embryos phenocopied the *FoxO1^{ECKO}* embryos and was similar to previous loss of function data (Lee et al., 2001). Yolk sacs harvested from both transgenic and control embryos confirmed the expression of exogenous *Sprouty4* and detection of YFP transcripts only in transgenic embryos (Figure S6).

Next, we collected total RNA from E8.25 transgenic YFP⁺ and control yolk sacs and embryos for analysis of arterial marker genes. The relative expression level of each arterial marker was normalized to relative endogenous *Sprouty4* in order to compare the effect of exogenous *Sprouty4* overexpression, and then compared between control and YFP⁺ transgenic

396   groups. Arterial markers, such as *Cx37*, *EphrinB2*, *Notch1*, *Hey1*, *Jagged1*, and *Dll4* were

397   significantly downregulated in the yolk sacs of transgenic embryos compared to controls (Figure

398   8C), while expression within the embryo proper of these markers was not significantly changed,

399   with the exception of *Jagged1* (Figure 8D). The expression of *Cx40* was not significantly

400   different between the control and transgenic groups in either the yolk sac or embryos (Figures

401   8C and D). Additionally, unlike in *FoxO1^{ECKO}* yolk sacs, expression of venous marker *EphB4*

402   was significantly down regulated in the yolk sac and *Coup-TFII* expression was significantly

403   increased in the transgenic embryos, suggesting that either Sprouty4 could have FOXO1

404   independent functions, or that abnormally high levels of *Sprouty4* may affect other processes.

405   These data, combined with our results showing that FOXO1 represses *Sprouty2/4* transcription,

406   indicates that FOXO1 acts as a key transcriptional regulator in arterial-venous specification by

407   repressing an antagonist of arterial specification.

408

DISCUSSION

410   Previously, using either through germline mutations or conditional approaches, several groups

411   demonstrated a requirement for FOXO1 in the early embryo, as these mutants featured failed

412   yolk sac remodeling and mid-gestation lethality (Sengupta et al., 2012, Furuyama et al., 2004,

413   Hosaka et al., 2004). In this paper, we investigated the role of FOXO1 within endothelial cells

414   prior to the onset of consistent circulation and overt vascular remodeling. It is well known that

415   arteriovenous specification and the arterial gene expression program are influenced by

416   hemodynamic forces (le Noble et al., 2004, le Noble et al., 2005, Wragg et al., 2014), but our

417   goal here was to determine whether FOXO1 functions in the endothelium before the onset of

418   hemodynamic signaling to affect arteriovenous patterning. Herein, we demonstrate that blood

419   flow is normal in *FoxO1^{ECKO}* mutants at these early stages, although heart failure and poor

420   circulation are evident by E9.5 (Figure 2). Others have shown that FOXO1 is not required for

421   heart development (Sengupta et al., 2012), and it is possible that heart failure in these embryos

17

422   is caused by the increased resistance of blood flow encountered in the unremodeled vitelline

423   vessels. It has also been noted that loss of FOXO1 causes allantois defects, preventing normal

424   allantois fusion and circulation to the placenta (Ferdous et al., 2011). We did not observe overt

425   defects in allantois fusion in $FoxO1^{ECKO}$ embryos (0/10 $FoxO1^{flox/flox};Tie2-cre^{Tg/+}$) (Table 1) and

426   observed only low penetrance of allantois fusion defects in (2/15) in the germline $FoxO1$ knock

427   out embryos, whereas 100% of all null or $FoxO1^{ECKO}$ embryos examined showed defects in yolk

428   sac remodeling, heart failure and mid-gestation lethality. Thus, it is likely that the heart failure

429   and lethality are caused by increased resistance to blood flow in vitelline vessels; however, the

430   reduction in $Dll4$ expression that we observed using the $Dll4-BAC-nlacZ$ reporter in $FoxO1^{ECKO}$

431   and germline null mutants suggest that further investigation of the consequence $Dll4$ loss in

432   allantois development is warranted.

433   In this study, we report that FOXO1 plays a previously unidentified role in regulating

434   arterial-specific gene expression prior to the onset of blood flow. Based on transcript expression

435   analyses, antibody immunostaining, and transgenic murine reporter experiments, we have

436   concluded that loss of $FoxO1$ causes a significant downregulation in $Flk1$ and other critical

437   arterial markers, including $Dll4$, in YS endothelial cells without affecting cell proliferation or cell

438   death. Further, our data demonstrate that FOXO1 directly binds to regulatory regions of $Sprouty$

439   2 and 4 in the yolk sac, and that FOXO1 acts as a direct repressor of $Sprouty$ 2 and 4 in

440   endothelial cells. Finally, we show that the overexpression of $Sprouty4$ in endothelial cells in

441    $vivo$ was sufficient to recapitulate impairments in both vascular remodeling and arterial cell fate

442   specification seen in $FoxO1$ mutants. Thus, these data indicate that repression of $Sprouty2/4$ by

443   FOXO1 is required to promote early, specification of arterial identity in the yolk sac prior to the

444   onset of robust embryonic circulation.

445   Interestingly, although we observed elevated $Sprouty$ $2/4$ transcripts in yolk sac

446   endothelial cells of $FoxO1$ null embryos, we found reduced $Sprouty$ 4 mRNA expression in non-

447   endothelial cells (CD31-) in the yolk sac, suggesting FOXO1 may act as activator for $Sprouty$ 4

18

448   in other cell types of the yolk sac. Several recent studies have shown that FOXO1 functions as

449   a transcriptional repressor in hepatocytes (Langlet et al., 2017) and pancreatic progenitor cells

450   (Jiang et al., 2017). Interestingly, in some instances co-factors have been identified that enable

451   FOXO1 to act as an activator or a repressor within the same tissues (Langlet et al., 2017). A

452   similar mechanism may explain the observed differences between endothelial and non-

453   endothelial cells within the yolk sac. It is not yet known whether a transcriptional co-factor in YS

454   endothelial cells is required for FOXO1 to act as a repressor, or if another mechanism accounts

455   for the opposite regulation of *Sprouty 4* in adjacent cell layers.

456   *FoxO1* loss did not appear to effect normal expression of pan-endothelial markers

457   *Pecam1*, *Tie2*, and other genes, but *Flk1/Vegfr2* was significantly reduced in both *FoxO1^{ECKO}*

458   and sorted germline mutant yolk sac endothelial cells. We also found that despite the reduction

459   in *Flk1/Vegfr2*, we did not observe changes in cell proliferation or cell viability, two process that

460   are directly regulated by VEGF-VEGFR signaling (Bernatchez et al., 1999). Sprouty factors

461   inhibit receptor tyrosine kinase (RTK) signaling, and Sprouty overexpression could cause a

462   reduction in *Flk1/Vegfr2* that is normally promoted by FLK1 or FGF receptor activation (Lee et

463   al., 2001, Casci et al., 1999). Indeed, we observed a reduction in *Flk1* transcripts when

464   *Sprouty4* was overexpressed in transgenic embryos, but also observed a strong effect on the

465   expression of other endothelial markers such as *Pecam*. It is also possible that the reduction of

466   *Flk1* expression seen in *FoxO1* mutants is a secondary consequence of disrupted arterial

467   specification, rather than a primary driver of this defect.

468   *Dll4* is among the earliest markers of arterial gene expression (Chong et al., 2011,

469   Wythe et al., 2013), but precisely how *Dll4* expression is initiated within the early yolk sac and

470   embryo remains poorly understood. While *Dll4* transcription was suggested to be regulated by 5'

471   binding of FOXC1/2 and β-catenin in its proximal promoter (Corada et al., 2010, Hayashi and

472   Kume, 2008, Seo et al., 2006), subsequent *in vivo* analysis showed that this region is not

473   sufficient to mediate expression (Wythe et al., 2013). Additionally, endothelial-specific loss of *β-*

474   *catenin* failed to alter *Dll4* expression in mice, or produce arteriovenous patterning defects

475   (Wythe et al., 2013). Furthermore, functional enhancers were found within intron 3 and

476   upstream at -12 and -16 kb that recapitulated the pattern of endogenous *Dll4* expression

477   (Sacilotto et al., 2013, Wythe et al., 2013), and these regions lacked conserved FOXC1/C2

478   binding sites, as well as TCF/LEF binding sites. In these current studies, we used a nuclear

479   localized LacZ reporter that recapitulates the normal expression pattern of *Dll4* (Herman et al.,

480   2018). Our data clearly showed that the reduction in *Dll4* expression was far more severe in the

481   yolk sac of $FoxO1^{ECKO}$ or null embryos than within the embryo proper. Similarly, the

482   overexpression of *Sprouty 4* throughout the embryo and yolk sac using an endothelial-specific

483   *Vegfr2/Flk1* promoter (Kappel et al., 1999, Ronicke et al., 1996, Fraser et al., 2005) indicated

484   that *Sprouty* overexpression did not alter arterial gene expression in the embryo, but

485   suppressed arterial transcripts in the yolk sac. The mechanism that explains the differential

486   activity of FOXO1 and SPROUTY2/4 within the vasculature of the yolk sac vs the embryo

487   proper remains unclear. Future experiments will be required to address numerous possible

488   explanations including differences in mesodermal cell lineages, differential binding to cofactors

489   and/or differences in post-translational modifications regulated by local cell-cell signaling.

490   One unresolved question from these studies is the relationship between abnormal

491   arteriovenous specification and failed vessel remodeling. Both arteriovenous identity and vessel

492   remodeling are regulated by hemodynamic forces, and AV specification relies on pathways that

493   respond to VEGF signaling (Fish and Wythe, 2015, Covassin et al., 2006, Weinstein and

494   Lawson, 2002, Fang et al., 2017). In $FoxO1^{ECKO}$, we detected a downregulation in

495   Flk1/VEGFR2. VEGFR2 and other VEGF receptors have been shown to act as shear stress

496   mechanosensors, signaling through downstream pathways such as the MEK-ERK kinase

497   cascade in response to changes in blood flow (Tzima et al., 2005, Baeyens and Schwartz,

498   2016). Thus, the downregulation of VEGFR2 in *FoxO1* mutant embryos could prevent ECs from

499   responding to normal blood flow signaling needed for vessel remodeling. Previously, our lab

500   showed that ECs within the vitelline arteries, but not the vitelline veins, migrate directionally in

501   response to hemodynamic changes in the yolk sac vasculature (Udan et al., 2013) so it is

502   possible that the loss of FOXO1 and/or the overexpression of *Sprouty2/4* interferes not only with

503   initial *Dll4* specification, but with the cell's ability to sense mechanical signaling that is necessary

504   to direct cell migration required for remodeling. Further work will be needed to better understand

505   the mechanisms leading both to early *Dll4* expression and those that regulate the cellular

506   responses needed for vessels to adapt to changes in blood flow.

507

508   **EXPERIMENTAL PROCEDURES**

509   **Animals and genotyping**

510   All animal experiments were conducted according to protocols approved by the Institutional

511   Animal Care and Use Committee of Baylor College of Medicine. *Ella-Cre* and *Tie2-Cre*

512   transgenic mice were purchased from Jackson Labs (# 003724 and 008863, respectively). *ε-*

513   *globin-KGFP* (Dyer et al., 2001), *FoxO1$^{flox/flox}$* mice (Paik et al., 2007), and *Dll4-BAC-nLacZ* mice

514   (Herman et al., 2018) were maintained and genotyped as previously described. *FoxO1* germline

515   knockout mice were generated by crossing the *FoxO1$^{flox/flox}$* mice to *Ella-Cre* mice (Lakso et al.,

516   1996). *Flk1-H2B::YFP* reporter mice were kindly provided by Dr. K. Hadjantonakis, Memorial

517   Sloan Kettering Cancer Center (Fraser et al., 2005).

518

519   **Immunostaining of whole or sectioned yolk sacs and LacZ staining**

520   E8.25 yolk sacs were fixed in 4% PFA, rinsed in PBS, permeabilized with 0.1% TritonX-100 for

521   1 hour, and blocked in 2% normal donkey serum/1% BSA for 5 hours. Yolk sacs were then

522   incubated with anti-PECAM1 antibody (BD Pharmingen, #550274; 1:100) overnight at 4°C. After

523   several PBS washes, yolk sacs were incubated with goat anti-rabbit antibody (Molecular

524   Probes, AlexaFluor 633,1:500) and DAPI (1:500) overnight at 4°C. Finally, yolk sacs were

525   rinsed in PBS and imaged using the Zeiss LSM510 META confocal microscope. Dissected yolk

526   sacs were cryosectioned at 20μm and sections were permeabilized and blocked, and incubated

527   with antibodies to either Caspase 3 (Cell Signaling #9661, 1:50); Connexin37 (ThermoFisher

528   Scientific #404200, 1:50); Connexin40 (ThermoFisher Scientific #364900, 1:50); eNOS (Santa

529   Cruz #sc-654, 1:50); Flk1 (Sigma #V1014, 1:100); or pHistone H3 (Millipore #06-570, 1:50)

530   overnight at 4°C. The secondary antibody incubation and image acquisition were performed as

531   described previously.

532

533   *Dll4-BAC-nLacZ* transgenic reporter were examined on *FoxO1* germline or *FoxO1^ECKO^* (*Tie2-*

534   *Cre^+/tg^;FoxO1^floxfloxl^*) backgrounds. E8.5 and E9.5 embryos were dissected in cold PBS and fixed

535   in 4% PFA. Embryos were then washed in X-gal rinse buffer (0.02% NP40, 0.01% sodium

536   deoxycholate; 4 x 15mins) and thereafter stained in x-gal solution [5mM $K_3Fe(CN)_6$, 5mM

537    $K_4Fe(CN)_6$, 0.01% sodium deoxycholate, 0.02% NP40, 2mM $MgCl_2$, 5mM EGTA, 1mg/ml X-gal]

538   at 37°C overnight. Embryos were then post-fixed in 4% PFA and then cleared in 50% and 70%

539   glycerol. Embryos from the same litter were processed and stained in a 20ml scintillation vial.

540   Stained embryos were photographed using the Axio ZoomV16 (Zeiss) stereo microscope and

541   thereafter genotyped.

542

543   **Quantification of *Flk1-H2B::YFP^+^* cell density, proliferation index and apoptotic index in**

544   **whole mount yolk sacs using FARSIGHT**

545   Acquired WT and ECKO yolk sac whole mount images (n>3 yolk sacs per genotype, n>3

546   regions of interest per yolk sac) were made into maximum intensity projections and separated

547   into individual RGB images: Red (pHistone-H3/Caspase 3), Green (Flk1-H2B::YFP) and Blue

548   (DAPI). Individual nuclei for Red, Green and Blue channels were segmented and quantified

549   using FARSIGHT, courtesy of Badri Roysam, University of Houston, which makes use of both

550   intensity and volume thresholds to distinguish two nuclei as separate. YFP^+^ cell density was

551   defined as the ratio of YFP^+^ nuclei to DAPI^+^ nuclei within that same field of view.

22

552   Proliferative/apoptotic index was defined as the ratio of PH3$^+$/ Caspase3$^+$ nuclei to the number

553   of DAPI$^+$ nuclei. Endothelial cell proliferative/apoptotic index was defined as the ratio of

554   YFP$^+$;PH3$^+$/Caspase3$^+$ double positive nuclei to the number of YFP$^+$ nuclei. The ratios were then

555   averaged over the various WT and ECKO yolk sac images.

556

557   **Live imaging and analysis of blood flow in *FoxO1* conditional knockout embryos**

558   *ε-globin-KGFP* reporter expressing GFP in primitive erythroblasts was examined in control and

559   ECKO background and litters were dissected at E8.5 or E9.5 for blood velocity analysis.

560   Embryos were dissected under a heated (37°C) dissection stage with warm dissection media

561   (DMEM/F-12, 10% FBS, 100 U/mL penicillin, and 100 µg/mL streptomycin). Embryos with intact

562   ectoplacental cone were placed in a glass bottomed culture chamber with culture medium (1:1

563   DMEM/F-12: rat serum, 100 U/mL penicillin, and 100 µg/mL streptomycin) and allowed to

564   recover in a 37°C incubator for 20 minutes. Embryos were then placed on a heated confocal

565   microscope stage (37°C) and imaged using the Zeiss LSM 5 LIVE laser scanning confocal

566   microscope, using the Achroplan 20X/0.45 NA objective. A 200-frame time lapse (in a 512x512

567   pixel frame) was acquired at 30-50 frames per second. Blood flow time lapses were acquired at

568   three different locations throughout the yolk sac per embryo, and at least three embryos of each

569   genotype were used for data collection. Individual blood cell velocities in each track were

570   determined from time lapse movies using Imaris. Individual blood cell velocities from three

571   different locations per embryo were averaged. Average heart beats per minute were calculated

572   by measuring the average time interval between peak velocities during the course of 5 cardiac

573   cycles in individual velocity profiles for each embryo imaged. Embryos were genotyped after

574   imaging, and blood velocities and heart beats per minute were averaged within WT and ECKO.

575

576   **Magnetic activated cell sorting of yolk sack endothelial cells**

23

577 To isolate E8.25 yolk sac endothelial cells, fresh yolk sacs were dissected in cold DMEM/F12

578 media without phenol red (ThermoFisher Scientific #21041025), individually placed in 100 μL of

579 cold TrypsinLE (Fisher Scientific #12605010), and kept on ice until all yolk sacs were harvested.

580 Embryos were used for genotyping. To dissociate yolk sacs into single cell suspension, gently

581 triturate with p200 pipette and incubate on ice for 5 minutes and repeat for a total of four times.

582 To inhibit the enzyme, add 1 mL of stop solution: media + 10% FBS (ThermoFisher Scientific

583 #26140079). The yolk sac cell suspensions were pelleted at 0.8 X 1000g for 5 minutes at 4

584 degrees Celsius. The pellets were resuspended in 90 μL of cell suspension buffer (PBS + 2%

585 FBS + 2 mM EDTA). 10μL of CD31 MicroBeads (Miltenyi Biotec #130-097-418) were added to

586 each yolk sac cell suspension and samples were incubated on ice for 15 minutes in the dark.

587 Cell mixtures were pelleted at 0.8 X 1000g for 5 minutes at 4 degrees Celsius and washed with

588 1mL of cell suspension buffer. Cell mixtures were once again pelleted at 0.8 X 1000g for 5

589 minutes at 4 degrees Celsius and resuspended in 200uL of cell suspension buffer. Cell mixtures

590 were passed through 40 μm cell strainers (Fisher Scientific #352340) into FACS tubes and

591 strainers were washed with 300 μL of cell suspension buffer. MS columns (Miltenyi Biotec #130-

592 041-301) were placed on OctoMACS separator and prepared according to manufacturer

593 instructions. Cell mixtures were individually passed through columns and the flow through was

594 reapplied through columns to maximize endothelial cell retention (CD31$^+$ population). Columns

595 were washed three times with 500 μL cell suspension buffer and all flow through was collected

596 (CD31$^-$ population). Bound cells were released from the columns by removal from magnetic

597 separator, and 1 mL of cell suspension buffer was applied to the columns and cells were flushed

598 using plunger into a 1.5 mL Eppendorf tube. Collected cells were then pelleted at 0.8 X 1000g

599 for 5 minutes at 4 degrees Celsius and resuspended in Trizol (Thermo Fisher 15596018). After

600 genotyping, CD31$^+$ and CD31$^-$ populations from two yolk sacs were combined and processed

24

601 for RNA isolation (QIAGEN RNeasy Micro Kit #74004), cDNA synthesis and qRT-qPCR as

602 described below.

603

604 **RNA isolation and qRT-PCR analysis**

605 Total RNA was isolated from pooled E8.25 yolk sacs dissected from either *Tie2-Cre$^{+/tg}$;*

606 *FoxO1$^{+/flox}$* or *Tie2-Cre$^{+/tg}$; FoxO1$^{flox/flox}$* embryos. Purified RNA was reverse transcribed

607 (ThermoFisher Scientific #11752-050) and gene expression analysis was performed using

608 TaqMan real-time assays for *FoxO1*, *Adm, Bmper, Vcam1*, and a panel of endothelial, arterial,

609 and venous markers (see Fig. 2D, E for gene list). The data were normalized to *Gapdh* (Pfaffl,

610 2001) and relative expression ratios between control and ECKO embryos were determined.

611 Endogenous *FoxO1* and *Sprouty*1-4 expression from pooled E8.25 yolk sacs (CD1 strain) was

612 also probed by TaqMan real-time assay, but expression was calculated as fold change relative

613 to *FoxO1*, which was set to 1.

614 Endogenous *Dll4* expression was measured in either germline *FoxO1* knockouts or

615 *FoxO1* [ECKO] embryos at E8.25. The allantois was used for genotyping and total RNA was

616 extracted from individual embryos and yolk sacs (n≥3) and probed for *Dll4* expression via

617 TaqMan assay and fold change of expression between controls and homozygous *FoxO1* [ECKO]

618 mutants, and statistical analysis were performed as described above.

619

620 **Chromatin Immunoprecipitation (ChIP) and qPCR**

621 To determine endogenous FOXO1 chromatin occupancy, E8.25 yolk sacs from CD1 embryos

622 were used for chromatin extraction. Freshly dissected yolk sacs were dissociated in ice cold

623 PBS with protease inhibitors and the tissue was then crosslinked with 1.5% formaldehyde,

624 followed by incubation with 125 mM glycine, and washed with PBS. After centrifugation, the

625 pellet was resuspended in cell lysis buffer (5 mM PIPES, pH 8; 85 mM KCl; 0.5% NP40). The

626 samples were spun and the pellet was resuspended in nuclear lysis buffer (50 mM Tris-HCl, pH

25

627   8.1; 10 mM EDTA; 1% SDS) and then sonicated on ice using a Bioruptor (Diagenode) to obtain

628   sheared chromatin ranging between 100–500 bp. ChIP was performed according to the

629   instructions for Magna ChIP kit (Millipore #17-10085) using 5 µg of anti-FOXO1 antibody

630   (Abcam #ab39670) or rabbit IgG (Millipore #12370). The cross links were then reversed, and

631   the purified DNA was then analyzed by qPCR in technical triplicates using SYBR green master

632   mix and the primers listed in Table S1 to measure the percentage of co-precipitating DNA

633   relative to input (% input) in *Sprouy2* and *Sprouty4* genomic regions.

634

635   **Cloning of *mSprouty2/4* promoter constructs and Luciferase Assay**

636   Genomic regions of ~2kb in length of murine *Sprouty2* and *Sprouty4* were PCR amplified using

637   primers listed in Table S1, and using BAC clones of C57BL6 genomic DNA as template DNA

638   (CH29-611D15, CH29-100M12, respectively; CHORI BAC/PAC resources). PCR fragments

639   were ligated into pCRII-TOPO vector, sequenced, and then subcloned into pGL3-Promoter

640   vector (Promega). H1299 cells (ATCC #CRL-5803) were maintained in DMEM media

641   supplemented with 10% FBS, 100 U/ml penicillin, and 100 µg/ml streptomycin. For transient

642   transfections, 50,000 cells were plated (48-well plate) and after 24 hours, each well was co-

643   transfected with 200 ng of *Sprouty2/Sprouty4* promoter construct, 10 ng of pRL-TK, and 125 ng

644   expression plasmid (pcDNA3-FOXO::FLAG, Addgene #13507) using manufacturer's

645   recommendations for lipofectamine 3000. The total amount of expression plasmid transfected

646   per well was kept constant with varying amounts of pcDNA3.1 vector. As a negative control, a

647   *FoxO1* plasmid encoding a deleted DNA binding domain (amino acid 208-220) was used

648   (Addgene #10694). After 24 hours, cells were lysed and analyzed for firefly and *Renilla*

649   luciferase activities according to the procedure outlined in the Dual-Glo luciferase assay system

650   (Promega #E2920). All luciferase assays were performed in triplicates and repeated at least

651   three times. Student's *t*-test was used to assess statistical significance ($P < 0.05$ was

652   considered statistically significant) and the averages and standard deviation from triplicate

653   samples from representative assays were shown.

654

655   **Transient endothelial-specific *Sprouty* expression in embryos**

656   A mouse *Sprouty4* cDNA clone (TransOmics clone BC057005) was used as a template to PCR

657   amplify the coding sequence with 5' *Sac*I and 3' *Pme*I restriction sites (5'

658   GAGCTCCCAGCCTCA TGGAGCCC 3' and 5' GTTTAAACTCAGAAAGGCTTGTCAGAC 3')

659   and subcloned into pCRIITOPO vector (S4-2). The internal ribosome entry site (IRES)

660   sequence was amplified from pIRES-hrGFP1a vector (Agilent Technologies) with 5' *EcoR*V and

661   3' *EcoR*I restriction sites using primers 5' CTATAGATATCACCCCCCTCTCCCTA 3' and 5'

662   GCATGAATTCGGTTGTGGCCATT ATCATCGTG 3' and subcloned into pCRIITOPO vector

663   (IRES-4). To assemble the final transgenic construct, clones S4-2 and IRES-4 were excised

664   with 5' *Ecl136*II and 3' *Not*I, and 5' *Not*I and 3' *Ecl136*II, respectively, and co-ligated into *Flk1*-

665   H2B/EYFP vector (kindly provided by Dr. K. Hadjantonakis, Memorial Sloan Kettering Cancer

666   Center) via a blunt-ended *Hind*III site. The *Flk1*-H2B/EYFP vector has a well characterized *Flk1*

667   promoter and intronic enhancer sequences which drive YFP expression in endothelial cells

668   (Fraser et al., 2005). All clones were verified by DNA sequencing and the final transgenic

669   construct was excised with 5' *Sal*I and 3' *Xba*I to purify a 4.5kb fragment for pronuclear

670   microinjection, which was performed at the BCM Genetically Engineered Mouse Core. Transient

671   transgenic embryos were dissected with yolk sac intact and initially screened for YFP

672   expression using confocal microscopy. Gross morphology of the embryo and yolk sac

673   vasculature was examined at E9.5 while arterial marker analysis (*C37*, *Cx40*, *Dll4*, *EphB2*,

674   *Hey1*) was performed at E8.25, at which point embryos and yolk sacs of YFP positive and

675   negative samples (n=3 each) were lysed in Trizol for RNA extraction. Transgene-positive

676   embryos were also confirmed via qRT-PCR for YFP expression (data not shown) and also

677   quantitating the ratio of exogenous over endogenous *mSprouty4* expression using transcript-

678   specific primers. Detection was via the Sybr-green or Taqman assay (for arterial markers) and

679   fold change of expression between YFP-positive and negative samples, and statistical analysis

680   were performed as previously described.

681

682

683   **FIGURE LEGENDS**

684   **Figure 1. *FoxO1^{ECKO}* results in vascular remodeling defects and lethality.** (A) Quantitative

685   RT-PCR for *FoxO1* expression in control and ECKO yolk sacs. *P*<0.01. (B and C) Bright field

686   images of E10.5 littermate control and *FoxO1^{ECKO}* embryos. Control and *FoxO1^{ECKO}* embryos

687   within the yolk sac at E8.5 (D and E), E9.5 (F and G), and E10.5 (H and I). Pericardial edema

688   (arrow), blood pooling in the heart (asterisk). (J) Pecam1 staining in E9.5 control and CKO yolk

689   sacs. Scale bar = 500μm.

690

691   **Figure 2. Vascular remodeling defects in *FoxO1^{ECKO}* embryos do not result from reduced**

692   **blood flow.** Primitive erythroblasts in circulation in wild type and CKO embryos were marked by

693   crossing to an *ε-globin-GFP* transgenic reporter. Representative still images of E8.5 wild type

694   (A), ECKO (B), E9.5 wild type (C), and ECKO (D) embryos. Individual blood cells from A-D

695   were tracked and velocity profiles are plotted in E-H. Quantification of the average blood velocity

696   are graphed in I and J (Mann-Whitney U test, p=0.005). Average heart rates quantified in wild

697   type and ECKO embryos at E8.5 (K) and E9.5 (L) (Kruskal-Wallis test, p=0.003). Bars in graphs

698   are means ± standard error.

699

700   **Figure 3. FOXO1 regulates FLK1 expression without affecting other endothelial genes or**

701   **endothelial cell viability prior to blood flow.** (A) Expression levels of endothelial genes by

702   quantitative RT-PCR. (B)Yolk sacs from control and *FoxO1^{ECKO}* at E8.25 were DAPI-stained and

703   labelled with *Flk1-H2B::YFP* transgene, which marks the nuclei of endothelial cells

704   (arrowheads). Whole mount phosphoHistone-H3 (PH3) (C) or activated Caspase3 (D) staining

705   of control and *FoxO1^{ECKO}* E8.25 yolk sacs co-labeled with *Flk1-H2B::YFP* transgene and DAPI.

706   (E) Immuno-labeling for endogenous Flk1 and Pecam1 in control and *FoxO1^{ECKO}* yolk sacs.

707   Scale bars = 50μm (B -E). (F) Comparison of *Pecam1* expression in MACS sorted CD31-,

708   CD31+, and combined control E8.25 yolk sac cells by qPCR. Relative *Pecam1* (G) and *Flk1* (H)

709   expression between WT and *FoxO1* null E8.25 MACS sorted CD31- and CD31+ yolk sac cells.

710

711   **Figure 4. Arterial marker expression is reduced in *FoxO1^{ECKO}* yolk sac.** (A) Quantitative RT-

712   PCR expression analysis in control and *FoxO1^{ECKO}* yolk sacs; arterial (red), venous (blue), and

713   endoderm markers. *$p<0.05$, **$p<0.01$, ***$p<0.001$, data are means ±S.E. (B) Immuno-labeling

714   of eNOS and FLK1 in control and *FoxO1^{ECKO}* yolk sacs. Scale bars = 20μm.

715

716   **Figure 5. Characterization of arterial defects in *FoxO1^{ECKO}* and germline mutants using**

717   **the *Dll4-BAC-nlacZ* reporter** (A and B, D and E) *nlacZ* reporter activity was detected in the

718   dorsal aorta [DA] and umbilical artery [UA] in E8.25 control, *FoxO1^{ECKO}*, and *FoxO1* null

719   embryos. Arrowheads point to yolk sac endothelial cells in posterior region of yolk sac plexus.

720   (C and F) *Dll4* expression in control, *FoxO1^{ECKO}*, and *FoxO1* null embryos and yolk sacs. n>3.

721   *$p<0.05$. (G and H, K and L) *nlacZ* reporter activity in E9.5 control, *FoxO1^{ECKO}*, and *FoxO1* null

722   yolk sac and embryo; VA = vitelline artery [arrow]; insets in G and H show yolk sacs only. (I and

723   J, M and N) *nlacZ* reporter activity in E9.5 control, *FoxO1^{ECKO}*, and *FoxO1* null; EC =

724   endocardium, DA = dorsal aorta, IAV = intersomitic arterial vessels, ACV = arterial cranial

725   vasculature. Scale bars for E8.25 panes = 200μm; E9.25 = 500μm.

726

727 **Figure 6. FOXO1 regulates *Sprouty2/4* expression in the yolk sac vasculature.** Quantitative

728 RT-PCR analysis in E8.25 control and *FoxO1^{ECKO}* yolk sacs for (A) known FOXO1 targets and

729 (B) *Sprouty* family members. (C) Quantitative RT-PCR of endogenous *Sprouty1-4* expression

730 relative to *FoxO1*. (D) Quantitative RT-PCR of *Sprouty2/4* in MACS sorted E8.25 CD31+ and

731 CD31- control and *FoxO1* null yolk sac cells.

732

733 **Figure 7. FOXO1 directly binds to endogenous *Sprouty2/4* promoters and represses**

734 ***Sprouty2/4* transcription.** (A) Genomic locus of mouse *Sprouty2* gene with FOXO1 binding

735 sites in red. (B and E) FOXO1 ChIP-PCR using E8.25 yolk sac chromatin. (C) Luciferase activity

736 of FOXO1 on *Sprouty2* promoter in H1299 cells. (D) Genomic locus of mouse *Sprouty4* gene

737 with FOXO1 binding sites in red. (F) Luciferase activity of FOXO1 on *Sprouty4* promoter in

738 H1299 cells. *$p<0.05$, **$p<0.01$, ***$p<0.001$. EV, empty vector.

739

740 **Figure 8. Transient overexpression of *Sprouty4* in endothelial cells phenocopies**

741 **conditional loss-of-function *FoxO1* mutants.** (A) Schematic of Sprouty4 overexpression

742 construct for pro-nuclei injection. (B) Brightfield image of E9.5 non-transgenic (control) and

743 transgenic embryo (TG); confocal imaging of TG embryo showing YFP fluorescence in yolk

744 sac. Note vessel remodeling in the control yolk sac (arrow). Quantitative RT-PCR of arterial

745 markers in control and TG yolk sacs (C) and embryos (D) (n=3). *$p<0.05$, **$p<0.01$, ***$p<0.001$.

746

747 **Table 1.** Allantois phenotype analysis in control, null and ECKO embryos at E9.5.

Table S1   Primer sequences used for genotyping, ChIP-qPCR, and cloning

Gene/allele			Primer sequences (5'-3')	Purpose
ChIP	*mSprouty2*	(-4051)	TTCCAGTCCTCCAAGCAATCTAG AGTGCCTCCAGGAAGGGAAT	ChIP-qPCR
ChIP	*mSprouty2*	(4479)	AATTAGCAAATGGCTCCCGG TTTGTGACTGTGCCATGAAGC	ChIP-qPCR
ChIP	*mSprouty2*	(5060)	TAGGGCGACTCAGTGGCTATC GACCGGAGTCAAAGGACCTTC	ChIP-qPCR
ChIP	*mSprouty2*	(6972)	CATTTGTGTGTTTTGGGGAGAGAT CGGCAGTTGGGTTGGAATTA	ChIP-qPCR
ChIP	*mSprouty4*	(8755)	GATCTCCATCCGAATTCCAAATG CTTGGTTCGGCAAAGGCGAGAAAC	ChIP-qPCR
ChIP	*mSprouty4*	(14942)	CCACCACAAAAGTTACCACAGAAG GATATCTTCTAGATCAGTAC	ChIP-qPCR
ChIP negative control			GAAACCCGAATCTACATTCCGTTCC CTGGATTAACCCGATTATACACC	ChIP-qPCR
Luc	*mSprouty2*	(-4051)	GTGTACACAGGTATACTCTAGTCACCAACCC GGGACTCGATGTTGCAATGAGATACTCAACTC	PCR cloning
Luc m	*Sprouty2*	(4479/5060)	GATCTGTGACAAGCAGTGCCTCTGCTCAG GCCACAAGGTGACTAATGTTGTCAAGATGG	PCR cloning
Luc	*mSprouty2*	(6972)	CATTCAGACCTAGCACTGTGATTCATGC CAGTGTTCAGCCAAACCAGGTAGGCCTTGA	PCR cloning
Luc	*mSprouty4*	(8755)	CAGCGGTTCACTTGAAGCTGCCTTGACAAG CTCTGCCTCCCAACTGCTGGGATTAAAG	PCR cloning
Luc	*mSprouty4*	(14942)	CTGTAGCTGTTTCTGACTTCTTGGCTAGC GGCTGAAGACTCATTGTAGAATGGGTCATG	PCR cloning
Endogenous	*mSpry4 cDNA*		GAAGCCTGTCCCTTGGTGCAGTTCAG CTGGTCAATGGGTAAGATGGTGAGTG	qRT-PCR
Exogenous	*mSpry4 cDNA*		GCGAGGTGCAGGAATTCGTTAAGCTCTCCC CTGGTCAATGGGTAAGATGGTGAGTG	qRT-PCR

748   * pGL3-Promoter

Table S2   **Taqman assays for Gene expression analysis**

FoxO1	Mm00490672_m1	*Hey1*	Mm00468865_m1
FoxO3a	Mm01185722_m1	*Hey2*	Mm00468865_m1
FoxO4	Mm00840140_g1	*Jagged 1*	Mm00496902_m1
Flk1 (Kdr)	Mm00840140_g1	*Nrp1*	Mm00435379_m1
PECAM1	Mm01242584_m1	*Nrp2*	Mm00803099_m1
Tie2 (Tek)	Mm01242584_m1	*CoupTFII*	Mm00772789_m1
Flt1	Mm00438980_m1	*EphB4*	Mm01201157_m1
Connexin 43	Mm00438980_m1	*AFP*	Mm00431715_m1
eNOS	Mm00435217_m1	*ADM*	Mm00437438_g1
Connexin 37	Mm00433610_s1	*BMPER*	Mm01175806_m1
EphrinB2	Mm01215897_m1	*Sprouty2*	Mm00442344_m1
Notch1	Mm00435249_m1	*Sprouty4*	Mm00442345_m1
Dll4	Mm00444619_m1		

ADAMS, R. H., WILKINSON, G. A., WEISS, C., DIELLA, F., GALE, N. W., DEUTSCH, U., RISAU, W. & KLEIN, R. 1999. Roles of ephrinB ligands and EphB receptors in cardiovascular development: demarcation of arterial/venous domains, vascular morphogenesis, and sprouting angiogenesis. *Genes Dev,* 13**,** 295-306.

AITSEBAOMO, J., PORTBURY, A. L., SCHISLER, J. C. & PATTERSON, C. 2008. Brothers and sisters: molecular insights into arterial-venous heterogeneity. *Circ Res,* 103**,** 929-39.

ALBERT, P. S., BROWN, S. J. & RIDDLE, D. L. 1981. Sensory control of dauer larva formation in Caenorhabditis elegans. *J Comp Neurol,* 198**,** 435-51.

BAEYENS, N. & SCHWARTZ, M. A. 2016. Biomechanics of vascular mechanosensation and remodeling. *Mol Biol Cell,* 27**,** 7-11.

BEARD, R. S., JR., HOETTELS, B. A., MEEGAN, J. E., WERTZ, T. S., CHA, B. J., YANG, X., OXFORD, J. T., WU, M. H. & YUAN, S. Y. 2020. AKT2 maintains brain endothelial claudin-5 expression and selective activation of IR/AKT2/FOXO1-signaling reverses barrier dysfunction. *J Cereb Blood Flow Metab,* 40**,** 374-391.

BERNATCHEZ, P. N., SOKER, S. & SIROIS, M. G. 1999. Vascular endothelial growth factor effect on endothelial cell proliferation, migration, and platelet-activating factor synthesis is Flk-1-dependent. *J Biol Chem,* 274**,** 31047-54.

CASCI, T., VINOS, J. & FREEMAN, M. 1999. Sprouty, an intracellular inhibitor of Ras signaling. *Cell,* 96**,** 655-65.

CHLENCH, S., MECHA DISASSA, N., HOHBERG, M., HOFFMANN, C., POHLKAMP, T., BEYER, G., BONGRAZIO, M., DA SILVA-AZEVEDO, L., BAUM, O., PRIES, A. R. & ZAKRZEWICZ, A. 2007. Regulation of Foxo-1 and the angiopoietin-2/Tie2 system by shear stress. *FEBS Lett,* 581**,** 673-80.

CHONG, D. C., KOO, Y., XU, K., FU, S. & CLEAVER, O. 2011. Stepwise arteriovenous fate acquisition during mammalian vasculogenesis. *Dev Dyn,* 240**,** 2153-65.

CLEAVER, O. & KRIEG, P. A. 1998. VEGF mediates angioblast migration during development of the dorsal aorta in Xenopus. *Development,* 125**,** 3905-14.

778   CORADA, M., NYQVIST, D., ORSENIGO, F., CAPRINI, A., GIAMPIETRO, C., TAKETO,
779   M. M., IRUELA-ARISPE, M. L., ADAMS, R. H. & DEJANA, E. 2010. The Wnt/beta-
780   catenin pathway modulates vascular remodeling and specification by upregulating
781   Dll4/Notch signaling. *Dev Cell,* 18**,** 938-49.
782   COVASSIN, L. D., VILLEFRANC, J. A., KACERGIS, M. C., WEINSTEIN, B. M. &
783   LAWSON, N. D. 2006. Distinct genetic interactions between multiple Vegf receptors are
784   required for development of different blood vessel types in zebrafish. *Proc Natl Acad Sci
785   U S A,* 103**,** 6554-9.
786   DANG, L. T. H., ABURATANI, T., MARSH, G. A., JOHNSON, B. G., ALIMPERTI, S.,
787   YOON, C. J., HUANG, A., SZAK, S., NAKAGAWA, N., GOMEZ, I., REN, S., READ,
788   S. K., SPARAGES, C., APLIN, A. C., NICOSIA, R. F., CHEN, C., LIGRESTI, G. &
789   DUFFIELD, J. S. 2017. Hyperactive FOXO1 results in lack of tip stalk identity and
790   deficient microvascular regeneration during kidney injury. *Biomaterials,* 141**,** 314-329.
791   DHARANEESWARAN, H., ABID, M. R., YUAN, L., DUPUIS, D., BEELER, D., SPOKES, K.
792   C., JANES, L., SCIUTO, T., KANG, P. M., JAMINET, S. S., DVORAK, A., GRANT,
793   M. A., REGAN, E. R. & AIRD, W. C. 2014. FOXO1-mediated activation of Akt plays a
794   critical role in vascular homeostasis. *Circ Res,* 115**,** 238-251.
795   DICKINSON, M. E., FLENNIKEN, A. M., JI, X., TEBOUL, L., WONG, M. D., WHITE, J. K.,
796   MEEHAN, T. F., WENINGER, W. J., WESTERBERG, H., ADISSU, H., BAKER, C.
797   N., BOWER, L., BROWN, J. M., CADDLE, L. B., CHIANI, F., CLARY, D., CLEAK,
798   J., DALY, M. J., DENEGRE, J. M., DOE, B., DOLAN, M. E., EDIE, S. M., FUCHS, H.,
799   GAILUS-DURNER, V., GALLI, A., GAMBADORO, A., GALLEGOS, J., GUO, S.,
800   HORNER, N. R., HSU, C. W., JOHNSON, S. J., KALAGA, S., KEITH, L. C.,
801   LANOUE, L., LAWSON, T. N., LEK, M., MARK, M., MARSCHALL, S., MASON, J.,
802   MCELWEE, M. L., NEWBIGGING, S., NUTTER, L. M., PETERSON, K. A.,
803   RAMIREZ-SOLIS, R., ROWLAND, D. J., RYDER, E., SAMOCHA, K. E., SEAVITT,
804   J. R., SELLOUM, M., SZOKE-KOVACS, Z., TAMURA, M., TRAINOR, A. G.,
805   TUDOSE, I., WAKANA, S., WARREN, J., WENDLING, O., WEST, D. B., WONG, L.,
806   YOSHIKI, A., INTERNATIONAL MOUSE PHENOTYPING, C., JACKSON, L.,
807   INFRASTRUCTURE NATIONALE PHENOMIN, I. C. D. L. S., CHARLES RIVER, L.,
808   HARWELL, M. R. C., TORONTO CENTRE FOR, P., WELLCOME TRUST SANGER,
809   I., CENTER, R. B., MACARTHUR, D. G., TOCCHINI-VALENTINI, G. P., GAO, X.,
810   FLICEK, P., BRADLEY, A., SKARNES, W. C., JUSTICE, M. J., PARKINSON, H. E.,
811   MOORE, M., WELLS, S., BRAUN, R. E., SVENSON, K. L., DE ANGELIS, M. H.,
812   HERAULT, Y., MOHUN, T., MALLON, A. M., HENKELMAN, R. M., BROWN, S.
813   D., ADAMS, D. J., LLOYD, K. C., MCKERLIE, C., BEAUDET, A. L., BUCAN, M. &
814   MURRAY, S. A. 2016. High-throughput discovery of novel developmental phenotypes.
815   *Nature,* 537**,** 508-514.
816   DIXIT, M., BESS, E., FISSLTHALER, B., HARTEL, F. V., NOLL, T., BUSSE, R. &
817   FLEMING, I. 2008. Shear stress-induced activation of the AMP-activated protein kinase
818   regulates FoxO1a and angiopoietin-2 in endothelial cells. *Cardiovasc Res,* 77**,** 160-8.
819   DUARTE, A., HIRASHIMA, M., BENEDITO, R., TRINDADE, A., DINIZ, P., BEKMAN, E.,
820   COSTA, L., HENRIQUE, D. & ROSSANT, J. 2004. Dosage-sensitive requirement for
821   mouse Dll4 in artery development. *Genes Dev,* 18, 2474-8.

DYER, M. A., FARRINGTON, S. M., MOHN, D., MUNDAY, J. R. & BARON, M. H. 2001. Indian hedgehog activates hematopoiesis and vasculogenesis and can respecify prospective neurectodermal cell fate in the mouse embryo. *Development,* 128**,** 1717-30.

DZIADEK, M. & ADAMSON, E. 1978. Localization and synthesis of alphafoetoprotein in post-implantation mouse embryos. *J Embryol Exp Morphol,* 43**,** 289-313.

FANG, J. S., COON, B. G., GILLIS, N., CHEN, Z., QIU, J., CHITTENDEN, T. W., BURT, J. M., SCHWARTZ, M. A. & HIRSCHI, K. K. 2017. Shear-induced Notch-Cx37-p27 axis arrests endothelial cell cycle to enable arterial specification. *Nat Commun,* 8**,** 2149.

FERDOUS, A., MORRIS, J., ABEDIN, M. J., COLLINS, S., RICHARDSON, J. A. & HILL, J. A. 2011. Forkhead factor FoxO1 is essential for placental morphogenesis in the developing embryo. *Proc Natl Acad Sci U S A,* 108**,** 16307-12.

FISCHER, A., SCHUMACHER, N., MAIER, M., SENDTNER, M. & GESSLER, M. 2004. The Notch target genes Hey1 and Hey2 are required for embryonic vascular development. *Genes Dev,* 18**,** 901-11.

FISH, J. E., CANTU GUTIERREZ, M., DANG, L. T., KHYZHA, N., CHEN, Z., VEITCH, S., CHENG, H. S., KHOR, M., ANTOUNIANS, L., NJOCK, M. S., BOUDREAU, E., HERMAN, A. M., RHYNER, A. M., RUIZ, O. E., EISENHOFFER, G. T., MEDINA-RIVERA, A., WILSON, M. D. & WYTHE, J. D. 2017. Dynamic regulation of VEGF-inducible genes by an ERK/ERG/p300 transcriptional network. *Development,* 144**,** 2428-2444.

FISH, J. E. & WYTHE, J. D. 2015. The molecular regulation of arteriovenous specification and maintenance. *Dev Dyn,* 244**,** 391-409.

FOSBRINK, M., NICULESCU, F., RUS, V., SHIN, M. L. & RUS, H. 2006. C5b-9-induced endothelial cell proliferation and migration are dependent on Akt inactivation of forkhead transcription factor FOXO1. *J Biol Chem,* 281**,** 19009-18.

FRASER, S. T., HADJANTONAKIS, A. K., SAHR, K. E., WILLEY, S., KELLY, O. G., JONES, E. A., DICKINSON, M. E. & BARON, M. H. 2005. Using a histone yellow fluorescent protein fusion for tagging and tracking endothelial cells in ES cells and mice. *Genesis,* 42**,** 162-71.

FUKUMOTO, M., KONDO, K., UNI, K., ISHIGURO, T., HAYASHI, M., UEDA, S., MORI, I., NIIMI, K., TASHIRO, F., MIYAZAKI, S., MIYAZAKI, J. I., INAGAKI, S. & FURUYAMA, T. 2018. Tip-cell behavior is regulated by transcription factor FoxO1 under hypoxic conditions in developing mouse retinas. *Angiogenesis,* 21**,** 203-214.

FURUYAMA, T., KITAYAMA, K., SHIMODA, Y., OGAWA, M., SONE, K., YOSHIDA-ARAKI, K., HISATSUNE, H., NISHIKAWA, S., NAKAYAMA, K., NAKAYAMA, K., IKEDA, K., MOTOYAMA, N. & MORI, N. 2004. Abnormal angiogenesis in Foxo1 (Fkhr)-deficient mice. *J Biol Chem,* 279**,** 34741-9.

GALE, N. W., DOMINGUEZ, M. G., NOGUERA, I., PAN, L., HUGHES, V., VALENZUELA, D. M., MURPHY, A. J., ADAMS, N. C., LIN, H. C., HOLASH, J., THURSTON, G. & YANCOPOULOS, G. D. 2004. Haploinsufficiency of delta-like 4 ligand results in embryonic lethality due to major defects in arterial and vascular development. *Proc Natl Acad Sci U S A,* 101**,** 15949-54.

GOETZ, J. G., STEED, E., FERREIRA, R. R., ROTH, S., RAMSPACHER, C., BOSELLI, F., CHARVIN, G., LIEBLING, M., WYART, C., SCHWAB, Y. & VERMOT, J. 2014. Endothelial cilia mediate low flow sensing during zebrafish vascular development. *Cell Rep,* 6**,** 799-808.

GONG, Y., YANG, X., HE, Q., GOWER, L., PRUDOVSKY, I., VARY, C. P., BROOKS, P. C. & FRIESEL, R. E. 2013. Sprouty4 regulates endothelial cell migration via modulating integrin beta3 stability through c-Src. *Angiogenesis,* 16**,** 861-75.

GRIDLEY, T. 2010. Notch signaling in the vasculature. *Curr Top Dev Biol,* 92**,** 277-309.

HAYASHI, H. & KUME, T. 2008. Foxc transcription factors directly regulate Dll4 and Hey2 expression by interacting with the VEGF-Notch signaling pathways in endothelial cells. *PLoS One,* 3**,** e2401.

HERMAN, A. M., RHYNER, A. M., DEVINE, W. P., MARRELLI, S. P., BRUNEAU, B. G. & WYTHE, J. D. 2018. A novel reporter allele for monitoring Dll4 expression within the embryonic and adult mouse. *Biol Open,* 7.

HERZOG, Y., GUTTMANN-RAVIV, N. & NEUFELD, G. 2005. Segregation of arterial and venous markers in subpopulations of blood islands before vessel formation. *Dev Dyn,* 232**,** 1047-55.

HERZOG, Y., KALCHEIM, C., KAHANE, N., RESHEF, R. & NEUFELD, G. 2001. Differential expression of neuropilin-1 and neuropilin-2 in arteries and veins. *Mech Dev,* 109**,** 115-9.

HOSAKA, T., BIGGS, W. H., 3RD, TIEU, D., BOYER, A. D., VARKI, N. M., CAVENEE, W. K. & ARDEN, K. C. 2004. Disruption of forkhead transcription factor (FOXO) family members in mice reveals their functional diversification. *Proc Natl Acad Sci U S A,* 101**,** 2975-80.

HUANG, H. & TINDALL, D. J. 2007. Dynamic FoxO transcription factors. *J Cell Sci,* 120**,** 2479-87.

HWA, J. J., BECKOUCHE, N., HUANG, L., KRAM, Y., LINDSKOG, H. & WANG, R. A. 2017. Abnormal arterial-venous fusions and fate specification in mouse embryos lacking blood flow. *Sci Rep,* 7**,** 11965.

JI, R. P., PHOON, C. K., ARISTIZABAL, O., MCGRATH, K. E., PALIS, J. & TURNBULL, D. H. 2003. Onset of cardiac function during early mouse embryogenesis coincides with entry of primitive erythroblasts into the embryo proper. *Circ Res,* 92**,** 133-5.

JIANG, Z., TIAN, J., ZHANG, W., YAN, H., LIU, L., HUANG, Z., LOU, J. & MA, X. 2017. Forkhead Protein FoxO1 Acts as a Repressor to Inhibit Cell Differentiation in Human Fetal Pancreatic Progenitor Cells. *J Diabetes Res,* 2017**,** 6726901.

JIRAMONGKOL, Y. & LAM, E. W. 2020. FOXO transcription factor family in cancer and metastasis. *Cancer Metastasis Rev,* 39**,** 681-709.

JONES, E. A., BARON, M. H., FRASER, S. E. & DICKINSON, M. E. 2004. Measuring hemodynamic changes during mammalian development. *Am J Physiol Heart Circ Physiol,* 287**,** H1561-9.

KAPPEL, A., RONICKE, V., DAMERT, A., FLAMME, I., RISAU, W. & BREIER, G. 1999. Identification of vascular endothelial growth factor (VEGF) receptor-2 (Flk-1) promoter/enhancer sequences sufficient for angioblast and endothelial cell-specific transcription in transgenic mice. *Blood,* 93**,** 4284-92.

KIM, Y. H., CHOI, J., YANG, M. J., HONG, S. P., LEE, C. K., KUBOTA, Y., LIM, D. S. & KOH, G. Y. 2019. A MST1-FOXO1 cascade establishes endothelial tip cell polarity and facilitates sprouting angiogenesis. *Nat Commun,* 10**,** 838.

KISANUKI, Y. Y., HAMMER, R. E., MIYAZAKI, J., WILLIAMS, S. C., RICHARDSON, J. A. & YANAGISAWA, M. 2001. Tie2-Cre transgenic mice: a new model for endothelial cell-lineage analysis in vivo. *Dev Biol,* 230**,** 230-42.

914 KONDRYCHYN, I., KELLY, D. J., CARRETERO, N. T., NOMORI, A., KATO, K., CHONG,
915   J., NAKAJIMA, H., OKUDA, S., MOCHIZUKI, N. & PHNG, L. K. 2020. Marcksl1
916   modulates endothelial cell mechanoresponse to haemodynamic forces to control blood
917   vessel shape and size. *Nat Commun,* 11**,** 5476.
918 KREBS, L. T., STARLING, C., CHERVONSKY, A. V. & GRIDLEY, T. 2010. Notch1
919   activation in mice causes arteriovenous malformations phenocopied by ephrinB2 and
920   EphB4 mutants. *Genesis,* 48**,** 146-50.
921 KREBS, L. T., XUE, Y., NORTON, C. R., SHUTTER, J. R., MAGUIRE, M., SUNDBERG, J.
922   P., GALLAHAN, D., CLOSSON, V., KITAJEWSKI, J., CALLAHAN, R., SMITH, G.
923   H., STARK, K. L. & GRIDLEY, T. 2000. Notch signaling is essential for vascular
924   morphogenesis in mice. *Genes Dev,* 14**,** 1343-52.
925 LAKSO, M., PICHEL, J. G., GORMAN, J. R., SAUER, B., OKAMOTO, Y., LEE, E., ALT, F.
926   W. & WESTPHAL, H. 1996. Efficient in vivo manipulation of mouse genomic
927   sequences at the zygote stage. *Proc Natl Acad Sci U S A,* 93**,** 5860-5.
928 LANGLET, F., HAEUSLER, R. A., LINDEN, D., ERICSON, E., NORRIS, T., JOHANSSON,
929   A., COOK, J. R., AIZAWA, K., WANG, L., BUETTNER, C. & ACCILI, D. 2017.
930   Selective Inhibition of FOXO1 Activator/Repressor Balance Modulates Hepatic Glucose
931   Handling. *Cell,* 171**,** 824-835 e18.
932 LAWSON, N. D., SCHEER, N., PHAM, V. N., KIM, C. H., CHITNIS, A. B., CAMPOS-
933   ORTEGA, J. A. & WEINSTEIN, B. M. 2001. Notch signaling is required for arterial-
934   venous differentiation during embryonic vascular development. *Development,* 128**,** 3675-
935   83.
936 LAWSON, N. D., VOGEL, A. M. & WEINSTEIN, B. M. 2002. sonic hedgehog and vascular
937   endothelial growth factor act upstream of the Notch pathway during arterial endothelial
938   differentiation. *Dev Cell,* 3**,** 127-36.
939 LE NOBLE, F., FLEURY, V., PRIES, A., CORVOL, P., EICHMANN, A. & RENEMAN, R. S.
940   2005. Control of arterial branching morphogenesis in embryogenesis: go with the flow.
941   *Cardiovasc Res,* 65**,** 619-28.
942 LE NOBLE, F., MOYON, D., PARDANAUD, L., YUAN, L., DJONOV, V., MATTHIJSEN,
943   R., BREANT, C., FLEURY, V. & EICHMANN, A. 2004. Flow regulates arterial-venous
944   differentiation in the chick embryo yolk sac. *Development,* 131**,** 361-75.
945 LEE, S. H., SCHLOSS, D. J., JARVIS, L., KRASNOW, M. A. & SWAIN, J. L. 2001. Inhibition
946   of angiogenesis by a mouse sprouty protein. *J Biol Chem,* 276**,** 4128-33.
947 LIU, Z. J., SHIRAKAWA, T., LI, Y., SOMA, A., OKA, M., DOTTO, G. P., FAIRMAN, R. M.,
948   VELAZQUEZ, O. C. & HERLYN, M. 2003. Regulation of Notch1 and Dll4 by vascular
949   endothelial growth factor in arterial endothelial cells: implications for modulating
950   arteriogenesis and angiogenesis. *Mol Cell Biol,* 23**,** 14-25.
951 LOBOV, I. B., RENARD, R. A., PAPADOPOULOS, N., GALE, N. W., THURSTON, G.,
952   YANCOPOULOS, G. D. & WIEGAND, S. J. 2007. Delta-like ligand 4 (Dll4) is induced
953   by VEGF as a negative regulator of angiogenic sprouting. *Proc Natl Acad Sci U S A,* 104**,**
954   3219-24.
955 LUCITTI, J. L., JONES, E. A., HUANG, C., CHEN, J., FRASER, S. E. & DICKINSON, M. E.
956   2007. Vascular remodeling of the mouse yolk sac requires hemodynamic force.
957   *Development,* 134**,** 3317-26.
958 MACK, J. J. & IRUELA-ARISPE, M. L. 2018. NOTCH regulation of the endothelial cell
959   phenotype. *Curr Opin Hematol,* 25**,** 212-218.
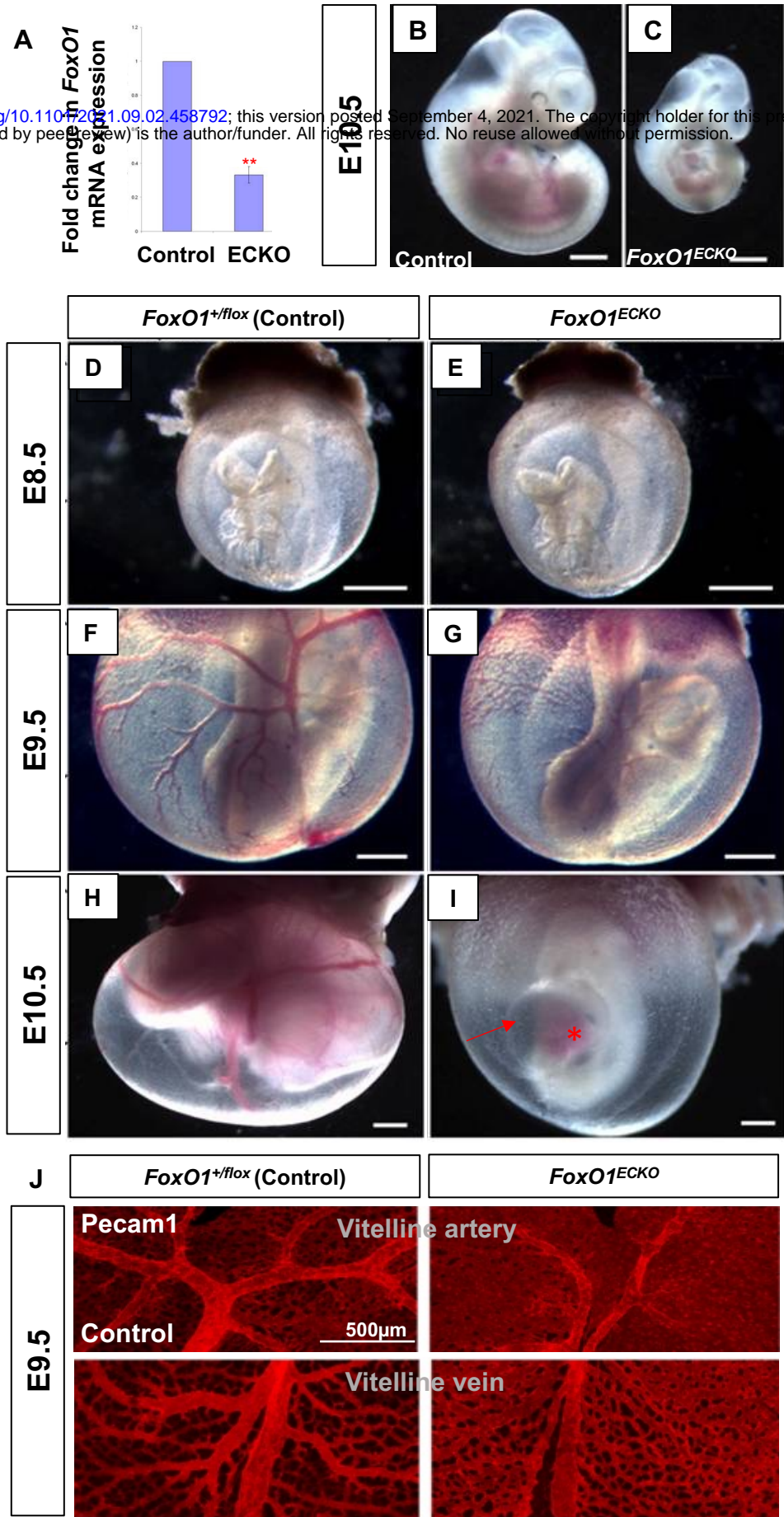
MACK, J. J., MOSQUEIRO, T. S., ARCHER, B. J., JONES, W. M., SUNSHINE, H., FAAS, G. C., BRIOT, A., ARAGON, R. L., SU, T., ROMAY, M. C., MCDONALD, A. I., KUO, C. H., LIZAMA, C. O., LANE, T. F., ZOVEIN, A. C., FANG, Y., TARLING, E. J., DE AGUIAR VALLIM, T. Q., NAVAB, M., FOGELMAN, A. M., BOUCHARD, L. S. & IRUELA-ARISPE, M. L. 2017. NOTCH1 is a mechanosensor in adult arteries. *Nat Commun,* 8**,** 1620.

MAILHOS, C., MODLICH, U., LEWIS, J., HARRIS, A., BICKNELL, R. & ISH-HOROWICZ, D. 2001. Delta4, an endothelial specific notch ligand expressed at sites of physiological and tumor angiogenesis. *Differentiation,* 69**,** 135-44.

MASUMURA, T., YAMAMOTO, K., SHIMIZU, N., OBI, S. & ANDO, J. 2009. Shear stress increases expression of the arterial endothelial marker ephrinB2 in murine ES cells via the VEGF-Notch signaling pathways. *Arterioscler Thromb Vasc Biol,* 29**,** 2125-31.

NIIMI, K., UEDA, M., FUKUMOTO, M., KOHARA, M., SAWANO, T., TSUCHIHASHI, R., SHIBATA, S., INAGAKI, S. & FURUYAMA, T. 2017. Transcription factor FOXO1 promotes cell migration toward exogenous ATP via controlling P2Y1 receptor expression in lymphatic endothelial cells. *Biochem Biophys Res Commun,* 489**,** 413-419.

OBI, S., YAMAMOTO, K., SHIMIZU, N., KUMAGAYA, S., MASUMURA, T., SOKABE, T., ASAHARA, T. & ANDO, J. 2009. Fluid shear stress induces arterial differentiation of endothelial progenitor cells. *J Appl Physiol (1985),* 106**,** 203-11.

PAIK, J. H., KOLLIPARA, R., CHU, G., JI, H., XIAO, Y., DING, Z., MIAO, L., TOTHOVA, Z., HORNER, J. W., CARRASCO, D. R., JIANG, S., GILLILAND, D. G., CHIN, L., WONG, W. H., CASTRILLON, D. H. & DEPINHO, R. A. 2007. FoxOs are lineage-restricted redundant tumor suppressors and regulate endothelial cell homeostasis. *Cell,* 128**,** 309-23.

PALIS, J. 2014. Primitive and definitive erythropoiesis in mammals. *Front Physiol,* 5**,** 3.

PFAFFL, M. W. 2001. A new mathematical model for relative quantification in real-time RT-PCR. *Nucleic Acids Res,* 29**,** e45.

POTENTE, M., URBICH, C., SASAKI, K., HOFMANN, W. K., HEESCHEN, C., AICHER, A., KOLLIPARA, R., DEPINHO, R. A., ZEIHER, A. M. & DIMMELER, S. 2005. Involvement of Foxo transcription factors in angiogenesis and postnatal neovascularization. *J Clin Invest,* 115**,** 2382-92.

RIDDELL, M., NAKAYAMA, A., HIKITA, T., MIRZAPOURSHAFIYI, F., KAWAMURA, T., PASHA, A., LI, M., MASUZAWA, M., LOOSO, M., STEINBACHER, T., EBNET, K., POTENTE, M., HIROSE, T., OHNO, S., FLEMING, I., GATTENLOHNER, S., AUNG, P. P., PHUNG, T., YAMASAKI, O., YANAGI, T., UMEMURA, H. & NAKAYAMA, M. 2018. aPKC controls endothelial growth by modulating c-Myc via FoxO1 DNA-binding ability. *Nat Commun,* 9**,** 5357.

RISAU, W. 1994. Angiogenesis and endothelial cell function. *Arzneimittelforschung,* 44**,** 416-7.

RISAU, W. & FLAMME, I. 1995. Vasculogenesis. *Annu Rev Cell Dev Biol,* 11**,** 73-91.

RONICKE, V., RISAU, W. & BREIER, G. 1996. Characterization of the endothelium-specific murine vascular endothelial growth factor receptor-2 (Flk-1) promoter. *Circ Res,* 79**,** 277-85.

RUDNICKI, M., ABDIFARKOSH, G., NWADOZI, E., RAMOS, S. V., MAKKI, A., SEPA-KISHI, D. M., CEDDIA, R. B., PERRY, C. G., ROUDIER, E. & HAAS, T. L. 2018. Endothelial-specific FoxO1 depletion prevents obesity-related disorders by increasing vascular metabolism and growth. *Elife,* 7.

1006 SACILOTTO, N., MONTEIRO, R., FRITZSCHE, M., BECKER, P. W., SANCHEZ-DEL-
1007   CAMPO, L., LIU, K., PINHEIRO, P., RATNAYAKA, I., DAVIES, B., GODING, C. R.,
1008   PATIENT, R., BOU-GHARIOS, G. & DE VAL, S. 2013. Analysis of Dll4 regulation
1009   reveals a combinatorial role for Sox and Notch in arterial development. *Proc Natl Acad*
1010   *Sci U S A,* 110**,** 11893-8.
1011 SENGUPTA, A., CHAKRABORTY, S., PAIK, J., YUTZEY, K. E. & EVANS-ANDERSON,
1012   H. J. 2012. FoxO1 is required in endothelial but not myocardial cell lineages during
1013   cardiovascular development. *Dev Dyn,* 241**,** 803-13.
1014 SEO, S., FUJITA, H., NAKANO, A., KANG, M., DUARTE, A. & KUME, T. 2006. The
1015   forkhead transcription factors, Foxc1 and Foxc2, are required for arterial specification
1016   and lymphatic sprouting during vascular development. *Dev Biol,* 294**,** 458-70.
1017 SHAY-SALIT, A., SHUSHY, M., WOLFOVITZ, E., YAHAV, H., BREVIARIO, F., DEJANA,
1018   E. & RESNICK, N. 2002. VEGF receptor 2 and the adherens junction as a mechanical
1019   transducer in vascular endothelial cells. *Proc Natl Acad Sci U S A,* 99**,** 9462-7.
1020 SHUTTER, J. R., SCULLY, S., FAN, W., RICHARDS, W. G., KITAJEWSKI, J.,
1021   DEBLANDRE, G. A., KINTNER, C. R. & STARK, K. L. 2000. Dll4, a novel Notch
1022   ligand expressed in arterial endothelium. *Genes Dev,* 14**,** 1313-8.
1023 SIEKMANN, A. F. & LAWSON, N. D. 2007. Notch signalling limits angiogenic cell behaviour
1024   in developing zebrafish arteries. *Nature,* 445**,** 781-4.
1025 SU, T., STANLEY, G., SINHA, R., D'AMATO, G., DAS, S., RHEE, S., CHANG, A. H.,
1026   PODURI, A., RAFTREY, B., DINH, T. T., ROPER, W. A., LI, G., QUINN, K. E.,
1027   CARON, K. M., WU, S., MIQUEROL, L., BUTCHER, E. C., WEISSMAN, I., QUAKE,
1028   S. & RED-HORSE, K. 2018. Single-cell analysis of early progenitor cells that build
1029   coronary arteries. *Nature,* 559**,** 356-362.
1030 SUN, X., CHEN, W. D. & WANG, Y. D. 2017. DAF-16/FOXO Transcription Factor in Aging
1031   and Longevity. *Front Pharmacol,* 8**,** 548.
1032 SWIFT, M. R. & WEINSTEIN, B. M. 2009. Arterial-venous specification during development.
1033   *Circ Res,* 104**,** 576-88.
1034 TANIGUCHI, K., ISHIZAKI, T., AYADA, T., SUGIYAMA, Y., WAKABAYASHI, Y.,
1035   SEKIYA, T., NAKAGAWA, R. & YOSHIMURA, A. 2009. Sprouty4 deficiency
1036   potentiates Ras-independent angiogenic signals and tumor growth. *Cancer Sci,* 100**,**
1037   1648-54.
1038 TZIMA, E., IRANI-TEHRANI, M., KIOSSES, W. B., DEJANA, E., SCHULTZ, D. A.,
1039   ENGELHARDT, B., CAO, G., DELISSER, H. & SCHWARTZ, M. A. 2005. A
1040   mechanosensory complex that mediates the endothelial cell response to fluid shear stress.
1041   *Nature,* 437**,** 426-31.
1042 UDAN, R. S., VADAKKAN, T. J. & DICKINSON, M. E. 2013. Dynamic responses of
1043   endothelial cells to changes in blood flow during vascular remodeling of the mouse yolk
1044   sac. *Development,* 140**,** 4041-50.
1045 WANG, H. U., CHEN, Z. F. & ANDERSON, D. J. 1998. Molecular distinction and angiogenic
1046   interaction between embryonic arteries and veins revealed by ephrin-B2 and its receptor
1047   Eph-B4. *Cell,* 93**,** 741-53.
1048 WEINSTEIN, B. M. & LAWSON, N. D. 2002. Arteries, veins, Notch, and VEGF. *Cold Spring*
1049   *Harb Symp Quant Biol,* 67**,** 155-62.

1050 WIETECHA, M. S., CHEN, L., RANZER, M. J., ANDERSON, K., YING, C., PATEL, T. B. &
1051   DIPIETRO, L. A. 2011. Sprouty2 downregulates angiogenesis during mouse skin wound
1052   healing. *Am J Physiol Heart Circ Physiol,* 300**,** H459-67.
1053 WILHELM, K., HAPPEL, K., EELEN, G., SCHOORS, S., OELLERICH, M. F., LIM, R.,
1054   ZIMMERMANN, B., ASPALTER, I. M., FRANCO, C. A., BOETTGER, T., BRAUN,
1055   T., FRUTTIGER, M., RAJEWSKY, K., KELLER, C., BRUNING, J. C., GERHARDT,
1056   H., CARMELIET, P. & POTENTE, M. 2016. FOXO1 couples metabolic activity and
1057   growth state in the vascular endothelium. *Nature,* 529**,** 216-20.
1058 WRAGG, J. W., DURANT, S., MCGETTRICK, H. M., SAMPLE, K. M., EGGINTON, S. &
1059   BICKNELL, R. 2014. Shear stress regulated gene expression and angiogenesis in
1060   vascular endothelium. *Microcirculation,* 21**,** 290-300.
1061 WYTHE, J. D., DANG, L. T., DEVINE, W. P., BOUDREAU, E., ARTAP, S. T., HE, D.,
1062   SCHACHTERLE, W., STAINIER, D. Y., OETTGEN, P., BLACK, B. L., BRUNEAU,
1063   B. G. & FISH, J. E. 2013. ETS factors regulate Vegf-dependent arterial specification.
1064   *Dev Cell,* 26**,** 45-58.
1065 XUE, Y., GAO, X., LINDSELL, C. E., NORTON, C. R., CHANG, B., HICKS, C., GENDRON-
1066   MAGUIRE, M., RAND, E. B., WEINMASTER, G. & GRIDLEY, T. 1999. Embryonic
1067   lethality and vascular defects in mice lacking the Notch ligand Jagged1. *Hum Mol Genet,*
1068   8**,** 723-30.
1069 YOU, L. R., LIN, F. J., LEE, C. T., DEMAYO, F. J., TSAI, M. J. & TSAI, S. Y. 2005.
1070   Suppression of Notch signalling by the COUP-TFII transcription factor regulates vein
1071   identity. *Nature,* 435**,** 98-104.
1072 ZHANG, H., GE, S., HE, K., ZHAO, X., WU, Y., SHAO, Y. & WU, X. 2019. FoxO1 inhibits
1073   autophagosome-lysosome fusion leading to endothelial autophagic-apoptosis in diabetes.
1074   *Cardiovasc Res,* 115**,** 2008-2020.
1075 ZHAO, Y., YANG, J., LIAO, W., LIU, X., ZHANG, H., WANG, S., WANG, D., FENG, J., YU,
1076   L. & ZHU, W. G. 2010. Cytosolic FoxO1 is essential for the induction of autophagy and
1077   tumour suppressor activity. *Nat Cell Biol,* 12**,** 665-75.
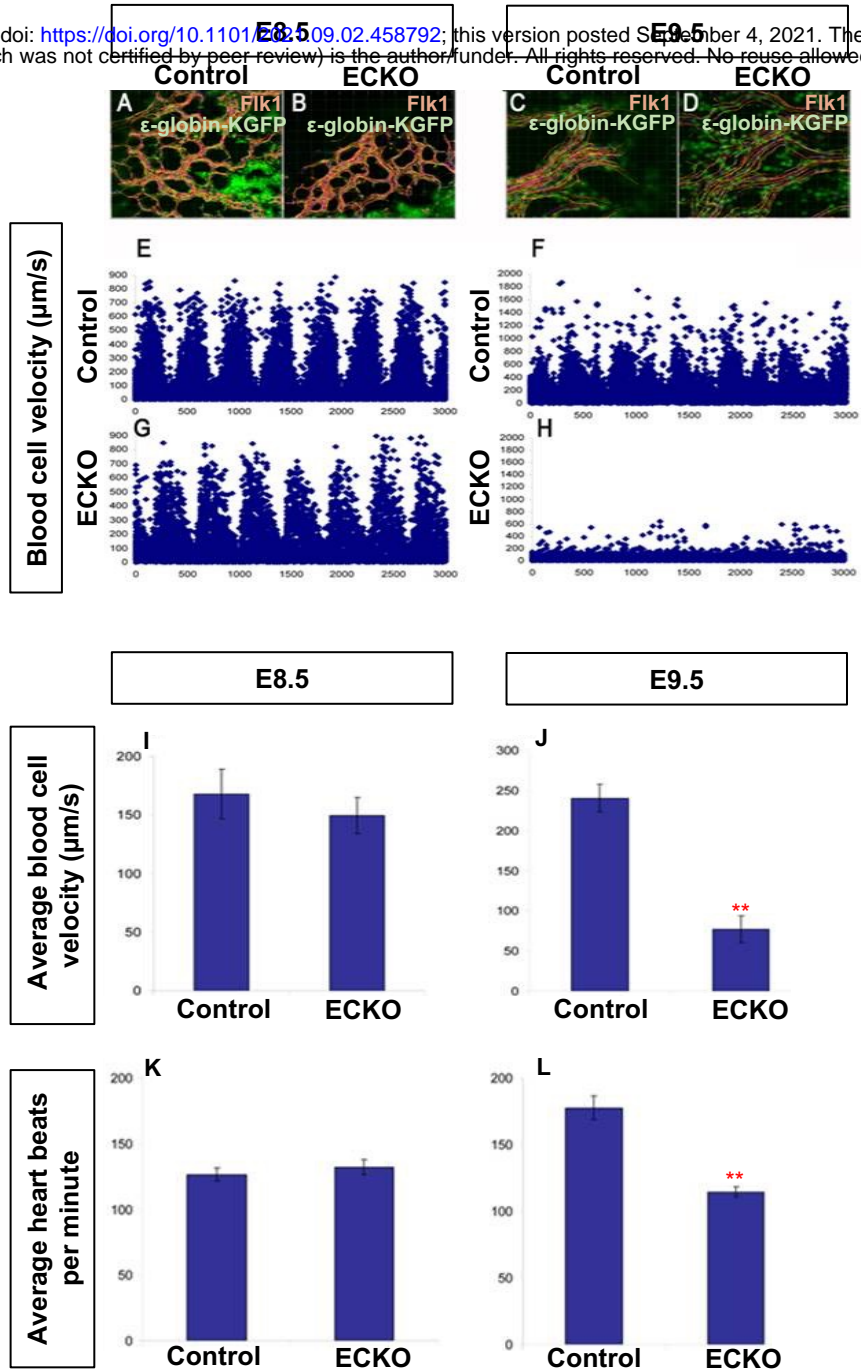1078

Fig. 1

A

Fold change in *FoxO1* mRNA expression

Control   ECKO

E10.5

B Control

C *FoxO1^ECKO^*

*FoxO1^+/flox^* (Control)	*FoxO1^ECKO^*

E8.5

D

E

E9.5

F

G

E10.5

H

I

J

*FoxO1^+/flox^* (Control)	*FoxO1^ECKO^*

E9.5

Pecam1   Vitelline artery

Control   500µm

Vitelline vein

Fig. 2

Table 1

	Genotype	Number	Percent of Total	Gross Allantois Defects	Percent of genotype
4 Litters	WT	16	31.37		
	FoxO1^{floxdel/+}	20	39.21		
	FoxO1^{floxdel/floxdel}	15	29.41	2	13.33
	Total	51			
6 Litters	*FoxO1*^{flox/+}	15	31.91		
	FoxO1^{flox/+};*Tie2-cre*^{Tg/+}	12	25.53		
	FoxO1^{flox/flox}	10	21.27		
	FoxO1^{flox/flox};*Tie2-cre*^{Tg/+}	10	21.27	0	0
	Total	47			

Fig. 3

A

B E8.25 yolk sac

C

D *Pecam1* expression

E *Flk1* expression

F E8.25 yolk sac

G Average YFP⁺ cell density

H E8.25 yolk sac

I E8.25 yolk sac

Fig. 4

Fig. 5

Fig. 6

A

B

C

D

Fig. 7

A

Mouse *Sprouty2* genomic locus

1 kb

- 4051   +4479 +5060   +6972

B

FOXO1 ChIP
E8.25 yolk sacs

% input

IgG
FOXO1

-4051 +4479 +5060 +6972 N.C.

C

- 4051   +4479 +5060   +6972

relative luminescence

NS

***

**

*

NS   NS

EV   FoxO1   FoxO1
ΔDBD   EV FoxO1   EV FoxO1

D

Mouse *Sprouty4* genomic locus

+14942

+8755   2

2 kb

E

FOXO1 ChIP
E8.25 yolk sacs

% input

IgG
FOXO1

+8755 +14942

F

+8755   +14942

relative luminescence

NS

NS

*

*

*

**

EV   FoxO1   FoxO1   EV   FoxO1   FoxO1
ΔDBD   ΔDBD

Fig. 8

A

B

C

D